MOLECULAR AND CELLULAR BIOLOGY, May 2003, p. 3186–3201 Vol. 23, No. 9
0270-7306/03/$08.00+0 DOI: 10.1128/MCB.23.9.3186–3201.2003


# Structural and Functional Analysis of Mutations along the Crystallographic Dimer Interface of the Yeast TATA Binding Protein

Haiping Kou, Jordan D. Irvin, Kathryn L. Huisinga, Madhusmita Mitra, and B. Franklin Pugh*

*Department of Biochemistry and Molecular Biology, The Pennsylvania State University, University Park, Pennsylvania 16803*

Received 18 November 2002/Returned for modification 23 December 2002/Accepted 5 February 2003

**The TATA binding protein (TBP) is a central component of the eukaryotic transcription machinery and is subjected to both positive and negative regulation. As is evident from structural and functional studies, TBP's concave DNA binding surface is inhibited by a number of potential mechanisms, including homodimerization and binding to the TAND domain of the TFIID subunit TAF1 (yTAF$_{II}$145/130). Here we further characterized these interactions by creating mutations at 24 amino acids within the *Saccharomyces cerevisiae* TBP crystallographic dimer interface. These mutants are impaired for dimerization, TAF1 TAND binding, and TATA binding to an extent that is consistent with the crystal or nuclear magnetic resonance structure of these or related interactions. In vivo, these mutants displayed a variety of phenotypes, the severity of which correlated with relative dimer instability in vitro. The phenotypes included a low steady-state level of the mutant TBP, transcriptional derepression, dominant slow growth (partial toxicity), and synthetic toxicity in combination with a deletion of the TAF1 TAND domain. These phenotypes cannot be accounted for by defective interactions with other known TBP inhibitors and likely reflect defects in TBP dimerization.**

Activation of eukaryotic genes is a multistep process, involving the coalescence of promoter-specific activators, chromatin-remodeling complexes, and components of the general transcription machinery at promoters. An important part of the activation process is the removal of inhibitors associated with latent activators, promoters, and the general transcription machinery. One component of the general transcription machinery that is subjected to substantial inhibition is the TATA binding protein (TBP) (reviewed in reference 75). Virtually all genes require TBP for function, and its association with promoters is generally linked to transcriptional activity (57, 63). Preventing unregulated promoter binding by TBP may be critical for preventing unregulated gene expression. TBP access might be prevented in part by nucleosome formation over the TATA box (43, 80). However, many quiescent genes are not derepressed upon histone depletion (83), indicating that other inhibitory mechanisms might prevent TBP from binding to promoters.

A number of proteins inhibit TBP function. These include the TAF1 (yTAF$_{II}$145/130) subunit of TFIID, NC2, Mot1, the Spt3/Spt8 subunits of SAGA, the Ccr4-Not complex, and a second molecule of TBP in the form of homodimers. Here we focus on two inhibitory interactions which are directed at TBP's concave surface: TBP dimerization and the TAF1 TAND domain.

TFIID is a multisubunit complex consisting of TBP and TAFs (19, 77, 78). TFIID is required for activated transcription but is intrinsically inhibitory toward TBP-TATA interactions (78). At least part of this inhibitory activity might reside within the amino-terminal TAND domain of the TFIID subunit, TAF1 (11, 52, 70). Mutagenesis studies have delineated *Drosophila* and yeast TANDs as two subdomains, I and II (52, 54). TAND II binds to TBP's convex surface in the vicinity of helix 2 (52). TAND I binds to the concave surface of TBP. Nuclear magnetic resonance (NMR) imaging of the *Drosophila* TAND I domain in complex with yeast TBP reveals that TAND I mimics the minor-groove structure of partially unwound TATA box DNA (65). The surface of TBP that interacts with the *Drosophila* TAND I domain has been partially mapped through mutagenesis (70), and it agrees well with the NMR structure of the complex. While the yeast and *Drosophila* TAND domains function similarly, it is striking that they are poorly (~30%) conserved, with yeast TAND being approximately half the size of *Drosophila* TAND (52). The structure of the yeast TAND I domain has not been determined, and where it interacts along TBP's concave surface has not been fully delineated. This is particularly intriguing given the small size of the yeast TAND I domain. It might be too small to occupy the entirety of TBP's concave surface.

If TAND inhibits TBP function in vivo, then deletion of this domain is expected to lead to an increase in transcription. However, very few genes increase in expression in a *taf1*(Δ*TAND*) strain (~60 out of ~6,000) (24). Mutations along TBP's concave surface result in widespread transcriptional derepression, which is augmented in a ΔTAND strain (24). These results suggest that TAND contributes to transcriptional inhibition but does not play a predominant role.

Self-association of TBP into dimers might provide a predominant means of inhibiting its concave DNA binding surface. Evidence that yeast and human TBPs autorepress their

* Corresponding author. Mailing address: Department of Biochemistry and Molecular Biology, The Pennsylvania State University, University Park, PA 16803. Phone: (814) 863-8252. Fax: (814) 863-8595. E-mail: bfp2@psu.edu.

DNA binding activities through dimerization comes from X-ray crystallography, pulldown assays, chemical cross-linking, gel filtration, analytical ultracentrifugation, and mutagenesis studies and has been inferred from its kinetic profile for DNA binding (22, 25–27, 42, 44, 45, 47, 69, 72, 81). Consistent with a dimer autorepression mechanism, TBP mutations that impair dimerization cause transcriptional derepression in vivo (24, 45). Their effect is dominant to wild-type TBP but is partially suppressed by wild-type TBP overexpression (45). TBP overexpression might drive unstable dimer mutants into somewhat more stable heterodimers with wild-type TBP.

Despite several observations that support a physiological role for TBP dimerization (45), the topic remains controversial (20). Ultimately, we wish to understand how a variety of TBP inhibitory mechanisms are coordinated to regulate TBP. A necessary step in this effort is the mapping of surfaces on TBP that are targeted for inhibition in vivo and the identification of factors responsible for that inhibition. In an effort to more completely examine the potential physiological significance of TBP dimerization, we mutated 24 amino acids that comprise the crystallographic dimer interface. Using in vitro pulldown and electrophoretic mobility assays, we characterized their abilities to dimerize, bind TAND, and bind TATA DNA. The binding data were in good agreement with the crystallographic and NMR structures of these or related complexes.

Next, we sought to determine whether mutations along the crystallographic dimer interface affect a variety of phenotypes in *Saccharomyces cerevisiae* that we previously linked to defects in dimerization (24, 45). These include increased TBP turnover, transcriptional derepression, partial dominant inhibition of cell growth (toxicity), and synthetic toxicity in a ΔTAND strain. With the collection of mutations throughout the dimer interface, we observed a correlation between these phenotypes and relative dimer stability measured in vitro. Mutations that knock out interfaces between TBP and other inhibitors did not give similar phenotypes. Taken together, the data provide further support for the notion that TBP dimerizes in vivo and is a physiologically important negative regulator of gene expression.

## MATERIALS AND METHODS

**Plasmids.** All TBP mutations were created by oligonucleotide-directed mutagenesis. The mutations and the integrity of the entire open reading frame were confirmed in both the bacterial and yeast expression vectors by DNA sequencing. *Escherichia coli* plasmids expressing the His-TBP mutants were designated pET16b-yTBP(xxx), where xxx indicates the mutation. The plasmid pGEX-TFIID-C, which encodes human GST-TBP(core), has been described previously (41). Plasmid pGEX-yTBP(181C) has been described previously (45). The plasmid pGEX-scTAF1(10-88) was constructed by PCR amplification of the *TAF1* gene and was inserted in frame with the glutathione *S*-transferase (GST)-coding sequence of pGEX-3X. Derivatives of this plasmid, pGEX-scTAF1(10-88, D66K) and pGEX-scTAF1(10-88, F23K, D66K), were constructed by oligonucleotide-directed mutagenesis. The integrity of the entire TAND coding region was verified by DNA sequencing. Plasmids expressing the $HA_3$-TBP mutants in *S. cerevisiae* were designated pCALF-T(xxx)(*PGK*), where CALF refers to the *CEN*/*ARS* origin, *LEU2* marker, $Flu_3$ (or $HA_3$) tagged; T indicates *TBP*; xxx is the mutation; and *PGK* is the promoter controlling $HA_3$-TBP expression. The plasmid is derived from pDP15-$flu_3$-yTBP (73), in which the *SPT15* promoter was replaced by the *PGK1* promoter, as described previously (45). The plasmid pCALF-T(K145E)(*GAL*) contains the *GAL10* promoter in place of the *PGK1* promoter as described previously (24). pADH1-lacZ contains the core (lacking the upstream activation sequence) *ADH1* promoter downstream of four glucose-repressible Gal4 binding sites (15). The plasmids TAF1/Ura, TAF1/Trp, and TAF1(ΔTAND)/Trp have been described previously as pYN1/*TAF145*, pYN2/*TAF145*, and pYN2/*taf145*(Δ*10-73*), respectively (52).

**Strains.** YTW22 [*MAT*α *ura3-52 trp1-*Δ*1 his3-*Δ*200 leu2-*Δ*1 lys2-801*$^{amber}$ *ade2-101*$^{ocher}$ Δ*spt15*::*TRP1*(pCW16-*TBP-WT*)] is a TBP plasmid shuffle strain (74). YPH252 (*MAT*α *ura3-52 trp1-*Δ*1 his3-*Δ*200 leu2-*Δ*1 lys2-801*$^{amber}$ *ade2-101*$^{ocher}$) is wild type for *TBP* (*SPT15*) and has been described previously (74). In vivo studies with *TAF1* and *taf1*(Δ*TAND*) employed the strain Y13.2 (*MAT*α *ura3-52 trp1-*Δ*63 leu2,3-112 his3-609* Δ*taf145* pYN1/*TAF145*), in which pYN1/*TAF145* was replaced by either pYN2/*TAF145* or pYN2/*taf145*(Δ*10-73)* by using the plasmid shuffle assay (52).

**Protein purification.** All His-tagged TBP mutants were purified as follows. Recombinant *E. coli* (BL21) cells (500 ml) were grown in YT medium containing 0.2 g of ampicillin per liter at 37°C to an optical density at 595 nm ($OD_{595}$) of 0.7 and induced with 20 mg of isopropylthio-β-D-galactoside per liter for 45 min at 30°C. Cells were harvested by centrifugation, washed and resuspended to a volume of 10 ml in lysis buffer (25 mM HEPES [pH 7.5], 200 mM potassium chloride, 12.5 mM magnesium chloride, 10% glycerol, 0.05 mM phenylmethylsulfonyl fluoride), and quickly frozen in liquid nitrogen. Cells were thawed and mixed with 0.8 mg of lysozyme per ml for 10 min at 4°C, with 2 M potassium chloride for 15 min, and with 0.2% IGEPAL-CA630 for 5 min. Extracts were sonicated to reduce viscosity and then centrifuged in an SS34 rotor (RC5C centrifuge) at 15,000 rpm for 30 min at 4°C. Supernatants were mixed with 10 mM imidazole and 0.5 ml of Ni-nitrilotriacetic acid–agarose for 60 min at 4°C. The slurry was then transferred to a column and then washed with wash buffer (20 mM HEPES [pH 7.5], 1 M potassium chloride, 12.5 mM magnesium chloride, 10% glycerol, 60 mM imidazole, 0.05 mM phenylmethylsulfonyl fluoride). TBP was eluted with TSB buffer (20 mM Tris-acetate [pH 7.5], 0.2 M potassium glutamate, 2 mM magnesium chloride, 20% glycerol, 0.05 mM phenylmethylsulfonyl fluoride) containing 1 M imidazole and dialyzed against TSB buffer containing 60 mM imidazole, 1 mM dithiothreitol, and 0.5 mM phenylmethylsulfonyl fluoride. TBP aliquots were frozen in liquid nitrogen and stored at −80°C. TBP was judged to be ~50% pure by sodium dodecyl sulfate-polyacrylamide gel electrophoresis (SDS-PAGE) followed by silver staining (see Fig. 2). Proteins concentrations were estimated from these gels by using highly purified TBP standards whose concentrations were determined by total amino acid analysis.

Human and yeast GST-TBP(core) were expressed from pGEX-TFIID-C and pGEX-yTBP(181C), respectively, and purified from 3 liters of recombinant *E. coli* cells as described above, with the following exceptions. Proteins were extracted with 1 M potassium chloride and 0.1% IGEPAL-CA630 (rather than 2 M and 0.2%, respectively). Glutathione agarose (1 ml) (Sigma) was used in place of nickel agarose. The resin was washed with H buffer (20 mM HEPES [pH 7.5], 2 mM magnesium chloride, 10% glycerol, 0.1 mM phenylmethylsulfonyl fluoride, and 1 mM dithiothreitol) containing 1 M potassium chloride (H1 buffer) and then with TSB buffer. The resin-bound GST-TBP(core) was aliquoted, quick-frozen in liquid nitrogen, and stored at −80°C.

GST-TAND was expressed from pGEX-scTAF1(10-88) and purified from recombinant *E. coli* DH5α cells as described above, with the following exceptions. Induction with isopropylthio-β-D-galactoside was for 2 h. Proteins were extracted with 0.1 M potassium chloride and 0.07% IGEPAL-CA630 (rather than 2 M and 0.2%, respectively). Glutathione agarose (0.75 ml) (Sigma) was used in place of nickel agarose. The resin was washed sequentially with H.35, H1, and then H.35 buffers. Proteins were eluted in H.35 containing 0.1 M reduced glutathione and dialyzed into H.35 buffer. Aliquots were frozen in liquid nitrogen and stored at −80°C. GST-TAND mutants were purified similarly. Proteins were judged to be approximately 90% pure by SDS-PAGE and silver staining.

**GST-TBP(core) pulldown assay.** Reaction mixtures contained 20 mM Tris-acetate (pH 7.5), 75 mM potassium glutamate, 4 mM magnesium chloride, 5% glycerol, 0.1 μg of bovine serum albumin per ml, 4 mM spermidine, 0.025% IGEPAL-CA630, 0.5 μg of heparin per ml, a 5 nM concentration of the indicated His-tagged TBP mutant, and 20 nM GST-TBP(core) or GST bound to 2 μl of glutathione agarose resin, in 500 μl. Reaction mixtures were incubated at 4°C for 45 min with mixing. Resins were washed three times, each with 500 μl of reaction buffer. Bound proteins were eluted and subjected to SDS-PAGE, and TBP was probed by immunoblotting with TBP antibodies. Reactions were typically performed at least six times, and representative data are shown. TBP was quantitated by densitometric scanning of autoradiograms. Relative pulldown was determined by subtracting local background and normalizing to a wild-type TBP pulldown present on the same gel.

**GST-TAND pulldown assay.** Reaction mixtures contained 20 mM Tris-Cl (pH 8.3), 150 mM potassium chloride, 12.5 mM magnesium chloride, 10% glycerol, 50 μg of bovine serum albumin per ml, 1 mM dithiothreitol, a 300 nM concentration of the indicated His-tagged TBP mutant, and 300 nM GST-TAND, GST-TAND(F23K D66K), or GST-TAND(D66K) bound to 10 μl of glutathione

agarose resin, in 100 μl. Reaction mixtures were incubated at 4°C for 30 min with mixing. Resins were washed three times, each with 500 μl of reaction buffer. Bound proteins were eluted and subjected to SDS-PAGE, and TBP was probed by immunoblotting with TBP antibodies. TAND was probed with GST antibodies and detected by enhanced chemiluminescence (ECL). All reactions were performed at least three times, and representative data are shown. TBP was quantitated by densitometric scanning of autoradiograms. Relative pulldown was determined by subtracting local background and normalizing to a wild-type TBP pulldown present on the same gel.

**Electrophoretic mobility shift DNA binding assay.** Reaction mixtures contained 22 mM Tris-acetate (pH 8.0), 60 mM potassium glutamate, 4 mM magnesium chloride, 10% glycerol, 5 μg of bovine serum albumin per ml, 1 mM dithiothreitol, 0.01% IGEPAL-CA630, 4 mM spermidine, 4 μg of poly(dG-dC) per ml, a 30 nM concentration of the indicated His-tagged TBP mutant, and ~2 nM $^{32}$P-labeled TATA double-stranded oligonucleotide (50 bp, 5′-CCCCGAC CGGGTGTGACAGTGAGGGGGC TATAAAAGGGGGTGGGGGCGCG-3′) in 10 μl. Reaction mixtures were incubated at 23°C for 40 min, and then 5-μl samples were loaded onto prerun (100 V, 40 min, 4°C) 15-cm native 6% (60.6:1 acrylamide/bisacrylamide ratio) polyacrylamide gels containing 1× TGM buffer (25 mM Tris-Cl [pH 8.3], 190 mM glycine, 1 mM EDTA, 5 mM magnesium acetate), 2.5% glycerol, and 0.5 mM dithiothreitol in running buffer containing 1X TGM. Electrophoresis was continued at 160 V (~35 mA) for 25 min at 4°C. Reactions were performed at least three times, and representative data are shown. The amount of shifted species was quantitated by phosphorimager analysis. Relative binding was determined by subtracting local background and normalizing to a wild-type TBP shift present on the same gel.

**Plasmid shuffle assay.** Strain YTW22 was transformed with the various pCALF-T(xxx)(*PGK*) plasmids. Deselection was performed on CSM-Leu plates containing 50 μg of uracil per ml. Cells were then restreaked onto plates containing the same medium with or without 1 mg of 5-fluoroorotic acid (5-FOA) per ml and incubated at 23, 30, or 37°C. Growth was examined daily and compared to that with wild-type TBP.

**Immunoblotting and β-galactosidase assay.** Strain YPH252 was transformed with the various pCALF-T(xxx)(*PGK*) plasmids and with pADH1-lacZ (β-galactosidase assay only) and plated on medium containing CSM-Leu plus 2%glucose (immunoblotting assay) or CSM-Ura-Leu plus 2%glucose (β-galactosidase assay). Cells were restreaked and used to inoculate 5 ml of liquid medium. For mutants that were partially toxic to cell growth, care was taken to use only the smaller colonies so as to avoid fast-growing revertants. Cells were grown at 30°C and 300 rpm. At an $OD_{600}$ of ~1.0, equivalent numbers of cells (~0.5 ml) were taken for immunoblot analysis. Cells were collected by centrifugation and lysed by vortexing with glass beads and standard SDS protein sample buffer. Hemagglutinin (HA)-tagged TBP mutants were separated from untagged wild-type endogenous TBP on a 10% polyacrylamide gel. TBP was then detected by immunoblotting with TBP antibodies and ECL. TBP levels were quantified by densitometry of autoradiographic films. A titration of recombinant TBP standards, spiked into a null extract, was used to ensure linearity of the quantitation.

β-Galactosidase assays were performed on equivalent numbers of cells (equivalent to 1 ml of cells with an $OD_{600}$ = 1.0), using the high sensitivity CPRG (chlorophenol red-β-D-galactopyranoside) substrate, as described previously (15). Data were normalized to a null TBP mutant, which expresses only amino acids 1 to 81 of TBP. Values represent averages from at least three experiments.

**Microarray analysis.** The experimental design, procedures, data filtering, and statistical analysis have been described previously (24). Fold changes ($log_2$) in gene expression for TBP(K145E) and TBP(K145E V161R) mutants are available from the authors upon request. Data for the other mutants are available from Chitikila et al. (24).

**Toxicity assay.** Strain YPH252 was transformed with the various pCALF-T(xxx)(*PGK*) plasmids and plated on CSM-Leu agar medium. Cells were then inoculated into CSM-Leu liquid medium, and the $OD_{600}$ during log phase was measured as a function of time. Appropriate dilutions of samples were made to remain within the linear range of the spectrophotometer. Doubling times were calculated from changes in OD readings as a function of time. Once cells reached an $OD_{600}$ of 1, samples were 10-fold serially diluted and 10 μl was spotted onto CSM-Leu agar plates. Growth was measured at 30°C and compared to that of strains harboring null TBP. Evaluation of the growth rates on the agar plates is described in Table 1.

**Synthetic toxicity assay.** Strain Y13.2 (containing pYN1/*TAF145*) was transformed with either pYN2/*TAF145* or pYN2/*TAF145*(Δ*10-73*). Cells were then streaked onto CSM-Trp plates containing 50 μg of uracil per ml for deselection of pYN1/*TAF145*. pYN1/*TAF145* was then eliminated by streaking onto CSM-Trp medium containing 1 mg of 5-FOA per ml. Cells were then transformed with pRS416 and plated on CSM-Ura-Trp medium. The four strains were then transformed with the various pCALF-T(xxx)(*PGK*) plasmids by using a high-efficiency lithium acetate transformation protocol (37) and then immediately diluted, and fivefold serially diluted samples (2.5 μl) were plated on CSM-Ura-Trp-Leu agar medium and incubated at 23, 30, or 37°C. Growth was examined daily as described in Table 1.

## RESULTS

**Mutations along TBP's concave surface decrease TBP self-association.** Within the crystallographic TBP dimer, 24 amino acids of one monomer reside within 4 Å of the other monomer (Fig. 1). Of these, 21 are identical in yeast and humans. These amino acids form a swath across TBP's concave surface and extend over the C-terminal stirrup. To identify amino acids important for dimerization, each was mutated to a bulky charged amino acid (arginine, lysine, or glutamic acid). Full-length yeast TBP mutants were expressed in bacteria as polyhistidine fusions and purified by using metal affinity chromatography (Fig. 2). The ability of the wild type and each TBP mutant to dimerize was assayed by using a GST pulldown assay in which GST was fused to the conserved core of either human or yeast TBP.

Since TBP has a tendency to aggregate nonspecifically, which would register as a false positive in this and other dimerization assays, it was essential that the interaction being measured along TBP's concave DNA binding surface was sensitive to a competing ligand known to interact with this surface, such as TATA DNA. As shown in Fig. 3A, TATA DNA inhibited the pulldown of TBP, while a corresponding TAAG mutant was less effective, indicating that the assay is specific.

The pulldown data for the TBP mutants are presented in Fig. 3B for human core and Fig. 3C for yeast core and are summarized in Table 1 and Fig. 4A. In control GST resin-only experiments, little or no binding of the wild type or any of the mutants was detected, further confirming that binding is specific. For the GST-TBP(core) pulldown, a range of interactions was observed with the TBP mutants, which were consistent between human core and yeast core. In general, we found the greatest loss of binding when amino acids that are buried within the crystallographic dimer interface were mutated. Mutation of amino acids that appeared to be solvent accessible in the crystallographic dimer had little or no effect on dimerization. The strong concordance between the crystallographic structure and the behavior of these mutants suggests that the TBP self-association being measured in this assay reflects interactions occurring in the crystallographic dimer.

**Mutations along TBP's concave surface decrease TBP-TAND interactions.** A GST-TAND pulldown assay was used to measure the interaction of amino acids 10 to 88 of the yeast TAF1 TAND domain with the various TBP mutants. This construct contains TAND I and II, both of which are required for TBP binding (54). To assess the specificity of binding, two TAND derivatives were generated, containing the F23K and D66K mutations or only the D66K mutation. The double mutant is defective in TBP binding (52). F23 resides within TAND I, and D66 resides within TAND II.

As shown in Fig. 5 and summarized in Table 1 and Fig. 4A, yeast TAND makes contact throughout the concave surface of TBP, in that mutations along this surface largely disrupted TAND binding. Mutations along TBP's convex C-terminal stirrup or along one edge of TBP's concave surface had little effect

TABLE 1. Properties of TBP mutants

| TBP | Stability[a] | | | Growth[b] at: | | | [TBP][c] | β-Gal[d] | Toxicity[e] | Synthetic toxicity[f] | | | |
|---|---|---|---|---|---|---|---|---|---|---|---|---|---|
| | TT | TF | TD | 23°C | 30°C | 37°C | | | | *TAF1* | | Δ*TAND* | |
| | | | | | | | | | | – | *TAF1* | – | *TAF1* |
| Null | | | | 0 | 0 | 0 | 0 | 1 | 1.9 | 6 | 6 | 4 | 6 |
| Wild type | 100 | 100 | 100 | 6 | 6 | 6 | 7 | 1 | 2.0 | 6 | 6 | 6 | 6 |
| Q68R | 58 | 90 | 100 | 5 | 6 | 5 | 6 | 5 | 2.2 | 4 | 4 | 6 | 4 |
| N69R | 9 | 20 | 20 | 0 | 0 | 0 | 0.4 | 190 | 3.2 | 2 | 4 | 0 | 2 |
| V71R | 18 | 90 | 5 | 0 | 0 | 0 | 0.7 | 81 | 4.5 | 2 | 4 | 0 | 2 |
| R98E | 23 | 80 | 50 | 4 | 4 | 4 | 4 | 1 | 2.1 | 5 | 6 | 6 | 6 |
| L114K | 41 | 10 | 5 | 0 | 0 | 0 | 7 | 7 | 3.9 | 6 | 5 | 4 | 5 |
| V122R | 23 | 40 | 10 | 0 | 0 | 0 | 4 | 44 | 2.1 | 6 | 6 | 2 | 4 |
| T124R | 25 | 50 | 10 | 0 | 0 | 0 | 4 | 31 | 2.7 | 3 | 3 | 1 | 3 |
| Q158R | 37 | 90 | 100 | 6 | 6 | 6 | 7 | 8 | 2.1 | 6 | 6 | 4 | 6 |
| N159R | 14 | 5 | 10 | 0 | 0 | 0 | 0.4 | 120 | 3.6 | 3 | 3 | 0 | 3 |
| V161R | 8 | 5 | 5 | 0 | 0 | 0 | 0.4 | 150 | 4.8 | 3 | 3 | 0 | 3 |
| R171E | 34 | 90 | 100 | 3 | 4 | 2 | 4 | 1 | 2.0 | 6 | 6 | 6 | 6 |
| F177R | 83 | 130 | 100 | 4 | 4 | 4 | 9 | 1 | 2.0 | 6 | 6 | 4 | 6 |
| G180R | 66 | 220 | 100 | 6 | 6 | 4 | 7 | 4 | 1.9 | 6 | 6 | 4 | 6 |
| T181R | 61 | 110 | 100 | 6 | 6 | 6 | 11 | 1 | 2.0 | 6 | 6 | 4 | 6 |
| S184R | 58 | 100 | 100 | 6 | 6 | 4 | 10 | 3 | 2.0 | 6 | 6 | 4 | 6 |
| E186R | 66 | 130 | 100 | 0 | 0 | 0 | 8 | 1 | 2.1 | 6 | 6 | 1 | 5 |
| F190R | 6 | 5 | 5 | 0 | 0 | 0 | 1.1 | 3 | 2.3 | 6 | 6 | 4 | 6 |
| I194R | 10 | 5 | 10 | 2 | 2 | 2 | 1.2 | 2 | 2.2 | 6 | 6 | 4 | 6 |
| R196E | 4 | 30 | 5 | 4 | 4 | 5 | 8 | 4 | 4.1 | 3 | 3 | 3 | 4 |
| K201E | 23 | 90 | 10 | 4 | 6 | 6 | 7 | 3 | 2.0 | 6 | 6 | 6 | 6 |
| V203E | 10 | 10 | 10 | 5 | 5 | 4 | 5 | 6 | 2.0 | 6 | 6 | 6 | 6 |
| L205R | 5 | 20 | 10 | 4 | 6 | 4 | 1.6 | 3 | 3.1 | 6 | 6 | 3 | 6 |
| V213R | 5 | 10 | 10 | 0 | 0 | 0 | 0.2 | 110 | 3.5 | 3 | 3 | 1 | 3 |
| T215R | 9 | 20 | 20 | 0 | 0 | 0 | 0.9 | 23 | 2.9 | 4 | 4 | 1 | 3 |

[a] TT, relative dimer stability (from Fig. 3C); TF, relative TBP-TAND stability (from Fig. 5 and reference 24); TD, relative TBP-TATA stability (from Fig. 6). Data are averaged from multiple repeats (scale of 0 to 100; wild-type value = 100).

[b] Relative colony size (scale of 0 to 6; null value = 0 and wild-type value = 6) on CSM-Leu solid agar plates at the indicated temperature, after shuffling out wild-type TBP. Relative values were confirmed by measuring doubling times in liquid medium.

[c] Relative concentration of HA-tagged TBP in vivo (endogenous untagged TBP value = 1.0), as measured in Fig. 7.

[d] Relative β-galactosidase activity (null TBP value = 1), as measured in Fig. 8.

[e] Measured in terms of doubling time (hours) for a strain (YPH252) harboring wild-type TBP, as described in Fig. 10.

[f] Relative colony size (0, no growth after 4 days; 1, pinpoint colonies after 4 days; 2, pinpoint colonies after 3 days; 3, pinpoint colonies after 2 days; 4, pinpoint colonies after 1 day; 5, colonies slightly smaller than those with wild-type TBP after 1 day; 6, colonies the same size as those with wild-type TBP) on CSM-Trp-Ura-Leu solid agar plates at 37°C in strain Y13.2 with the indicated *TAF1* alleles [*TAF1*, wild type, Δ*TAND*, *TAF*1(Δ10–88)], as described in Fig. 11. Essentially identical results were obtained at 30 and 23°C (data not shown).

(Fig. 4B). Overall there was a remarkable concordance of the mutagenesis data with what was predicted from the NMR and mutagenesis data for the *Drosophila* TAND-TBP complex (65, 70). Despite low sequence conservation, yeast TAND appears to be contacting TBP's concave surface in a manner similar (but probably not identical) to that for *Drosophila* TAND I.

**Mutations along TBP's concave surface decrease TATA binding.** A substantial portion of the dimer interface overlaps with TBP's DNA binding surface, and dimerization and DNA binding are competitive events (Fig. 3A). An electrophoretic mobility shift assay was performed to measure TATA binding by the various mutants (Fig. 6; summarized in Table 1 and Fig. 4A). As expected from the structure (48, 50), mutation of buried or bonded amino acids along the concave surface of TBP resulted in a loss of DNA binding, while mutation of other amino acids had little effect. The one exception was K201, which does not appear to contact DNA in the crystal structure but is nonetheless important for binding. Similar observations for this and other equivalent mutations throughout the DNA binding surface of TBP have been previously reported (4, 17, 61, 76, 84).

**Amino acids along TBP's crystallographic dimer interface are important for growth.** As a first step towards assessing the phenotypes of mutations along TBP's crystallographic dimer interface, we examined whether such mutants could support cell viability as the sole source of TBP. Yeast strain YTW22, harboring a deletion of the chromosomal *TBP* (*SPT15*) gene and providing wild-type *TBP* on a Ura-marked plasmid, was used to exchange the wild-type TBP with the mutant TBPs by plasmid shuffling. As summarized in Table 1 and Fig. 4A, mutations along the concave surface of TBP generally failed to support growth. In general, mutations on the convex portion of the dimer interface had little effect, with the exception of the TFIIB-defective E186R mutation, which failed to support growth, and R171E and F177R, which caused slow growth. R171 and F177 have genetic interactions with *SPT3* (34).

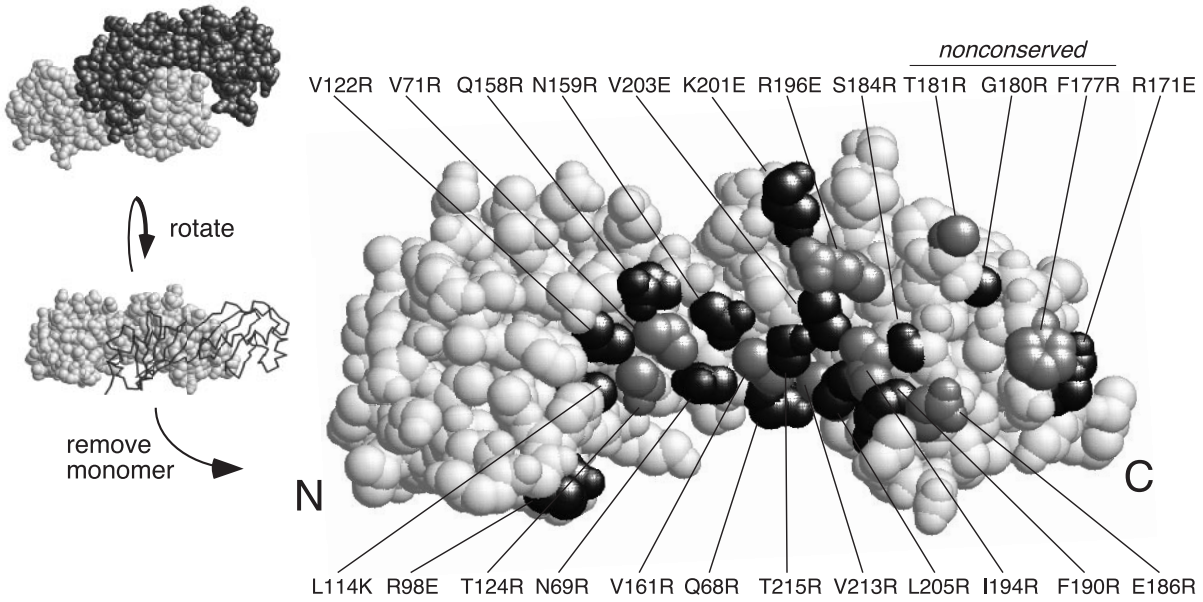


FIG. 1. Amino acids within the crystallographic dimer interface. Shown is a space-filling representation of a TBP monomer (22). Side chains that are within 4 Å of the other monomer in the dimer crystal structure are shaded (either black or gray). N and C refer to the amino-terminal and carboxy-terminal stirrups, respectively.

**In vivo steady-state levels of TBP mutants correlate with dimer stability.** Using a limited number of mutants, we previously reported a correlation between TBP dimer stability and steady-state levels of the TBP mutants in vivo (45). Gal shutoff experiments indicated that these mutants are likely to be more rapidly degraded, whereas wild-type TBP is stable (45). To examine the in vivo stability of TBP mutated along its crystallographic dimer interface, each mutant was HA tagged on its amino terminus and expressed under the control of the highly active *PGK1* promoter in a strain (YPH252) containing a normal chromosomal copy of the TBP gene (for cell viability). Under these conditions wild-type HA-TBP is overexpressed by approximately 10-fold. As shown in Fig. 7A and summarized in Table 1 and Fig. 4A, the TBP mutants displayed a range of steady-state levels in vivo relative to that of endogenous wild-type TBP.

Despite the possibility that defective interactions with a number of factors could differentially contribute to the steady-state levels of TBP, there was a strong correlation with dimer stability measured in vitro (Fig. 7B). These results provide further support for the notion that dimerization protects TBP from degradation. Previously, we presented evidence indicating that neither DNA nor TAND binding was likely to be primarily responsible for protecting TBP (24, 45). A subset of the mutants were also tested in a *spt3*Δ strain and found to be present at ratios similar to those found in wild-type cells, indicating that potential defects in Spt3 (and likely SAGA) interactions are unlikely to account for the rapid turnover of the TBP mutants (data not shown). Also, TBP mutants K145E and F182V, which are defective in Mot1 and NC2 interactions, respectively, were expressed at near-normal levels (reference

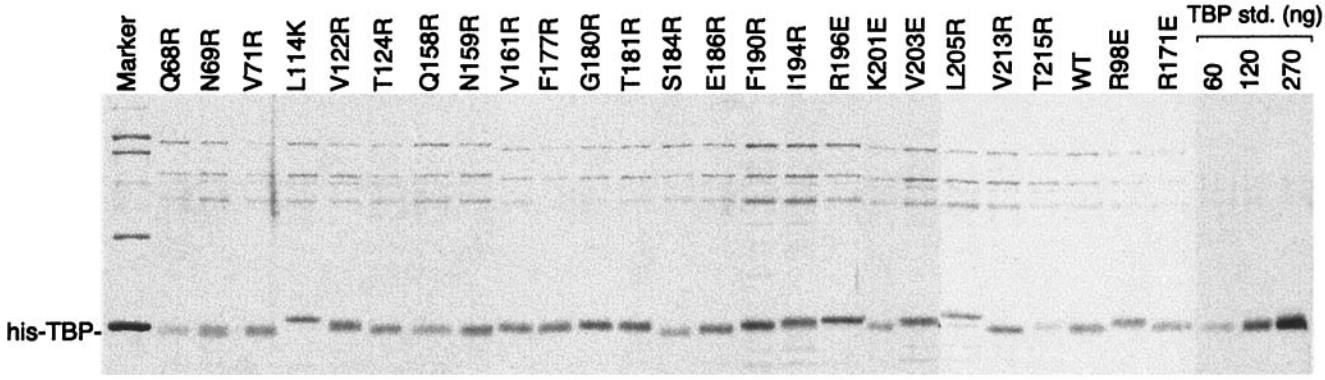


FIG. 2. Purification of recombinant His-tagged yeast TBP mutants. Proteins were purified from recombinant *E. coli* by using nickel-agarose, as described in Materials and Methods. Proteins were electrophoresed on a 10% polyacrylamide gel and stained with silver. WT, wild type; std., standard.

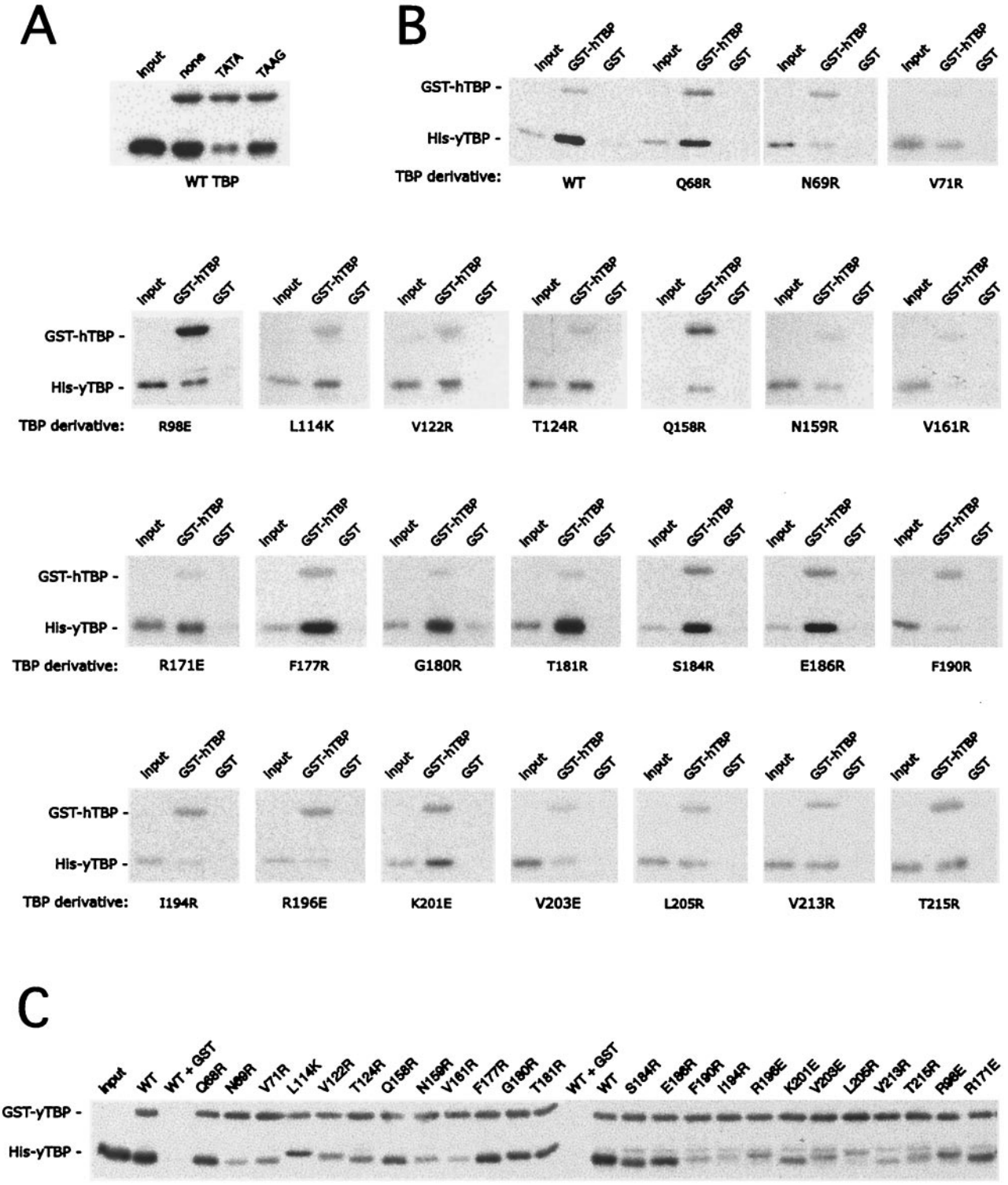


FIG. 3. Dimerization of TBP mutants. (A) Pulldown assay using 20 nM human GST-TBP(core) bound to glutathione resin and 5 nM yeast His-TBP. Reactions also included 100 nM of either TATA or mutant TAAG 28-bp DNA double-stranded oligonucleotide, as indicated. Resins were washed, and proteins were eluted and analyzed by SDS-PAGE. His-TBP was detected by immunoblotting with polyclonal antibodies directed against yeast TBP. Shown is 5% of the input. WT, wild type. (B) Same as panel A except the indicated yeast His-TBP mutants were used. Shown is 2% of the input. (C) Same as panel A except that reaction mixtures contained 20 nM yeast GST-TBP(181C) core and a 45 nM concentration of the indicated yeast His-TBP mutants. Input is shown at 7%. Where indicated, equal moles of GST were used in place of GST-TBP core. Yeast TBP antibody reacts poorly with yeast TBP core and very poorly with human TBP core.

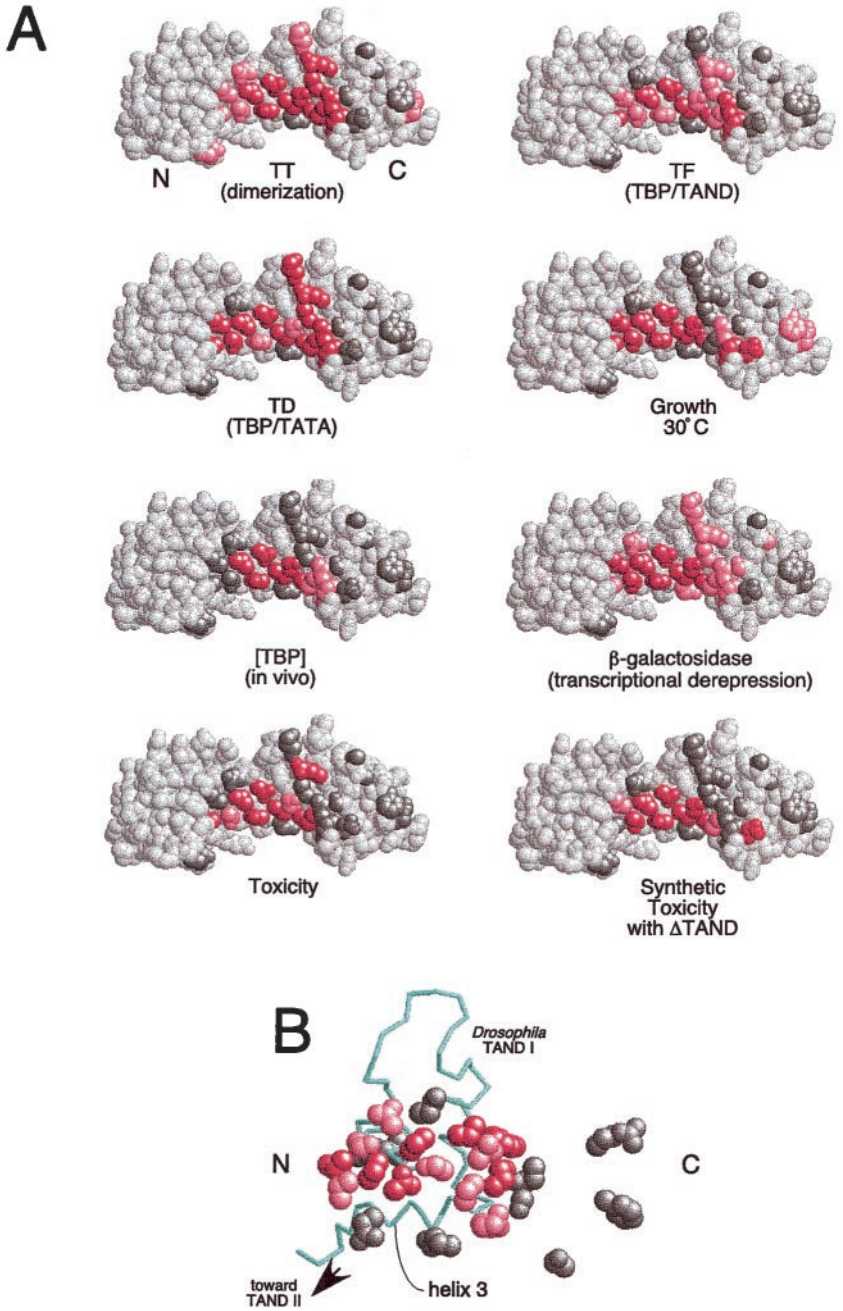


FIG. 4. Summary of the properties of mutations along TBP's crystallographic dimer interface. (A) Shown are space-filling models of TBP monomers in the orientation shown in Fig. 1. N and C refer to the amino-terminal and carboxy-terminal stirrups, respectively. Each model is a summary derived from Table 1, in which each of the 24 tested amino acid side chains are color coded if mutations at these sites cause severe (red), moderate (pink), or no (gray) deviations from wild-type behavior. Since V71E but not V71R is defective for TAND binding (24), this residue was colored red. (B) The NMR structure of the *Drosophila* TAF1 TAND I backbone (from amino acid 19 to 77) is shown in the context of a space-filling representation of yeast TBP amino acid side chains that were used in this study (65). The color scheme is the same as that used in panel A. The view is that of panel A but rotated forward such that the TBP stirrups point inward and the convex seat of the saddle is facing outward.

24 and data not shown), indicating that Mot1 and NC2 were not primarily responsible for preventing TBP turnover.

**Mutations along TBP's concave surface cause transcriptional derepression.** Previously, we and others identified amino acids along the concave surface of TBP that when mutated lead to transcriptional derepression (15, 21, 24, 36, 45). The level of derepression correlated with dimer instability (24, 45). To determine whether a similar correlation held with a more complete set of mutants, we employed the same system, which included the use of a *lacZ* reporter gene fused to the core (enhancerless) *ADH1* promoter (15). Artificial Gal4p binding sites are located upstream of the promoter. Cells (YPH252

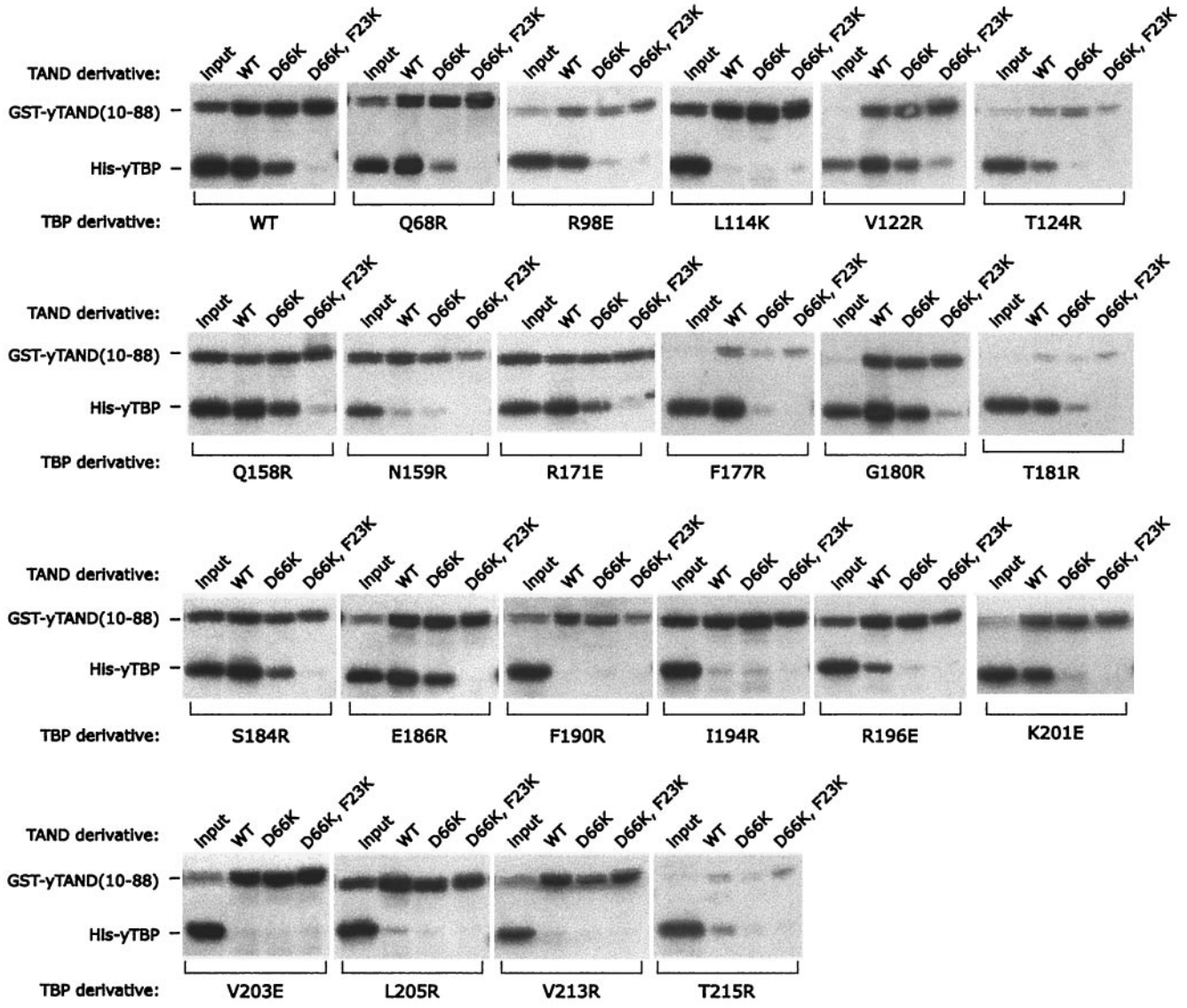


FIG. 5. Interaction of TAND with TBP mutants. His-tagged TBP mutants (300 nM), as indicated below each panel, were incubated with glutathione resin containing a 300 nM concentration of either GST-yTAND(10-88) (wild type [WT]), GST-TAND(D66K), or GST-TAND(F23K D66K). Resins were washed, and proteins were eluted and analyzed by SDS-PAGE. TBP was detected by immunoblotting with polyclonal antibodies directed against TBP. The GST-TAND derivatives were detected with GST antibodies. The GST-TAND signal is not comparable between panels, since different lots of GST antibodies were used for some. Shown in each panel is 10% of the input. Mutants not shown here are presented in reference 24.

derivatives) were grown in glucose medium, thereby subjecting the reporter to glucose-mediated repression. TBP mutants were expressed under the control of the *PGK1* promoter, as described above.

Mutations along TBP's crystallographic dimer interface led to varying degrees of transcriptional derepression, which inversely correlated with dimer stability (Fig. 8 and Table 1). Eight mutations (N69R, V71R, V122R, T124R, N159R, V161R, V213R, and T215R) caused between 20- and 200-fold increases in β-galactosidase activity. All eight cluster along the deepest part of TBP's concave surface (illustrated in red in Fig. 4A). Surrounding these amino acids is a second tier (illustrated in pink in Fig. 4A) that displayed modest derepression. Mutations along the convex surface of the crystallographic dimer interface had little effect. This collection of mutations demarcate a strong inhibitory region along TBP's concave surface. It is remarkable that a fairly robust correlation was observed between transcriptional repression and dimer stability, particularly since varying degrees of defects in DNA binding are expected to dampen the observed level of derepression.

TBP's nonconserved amino-terminal domain has been implicated as an inhibitor of TBP-TATA interactions (55, 60) and thus could conceivably inhibit TBP's concave surface. To examine whether such an interaction contributes to inhibition of the *lacZ* reporter, a TBP derivative (181C) which lacks the nonconserved amino-terminal domain of TBP was overex-

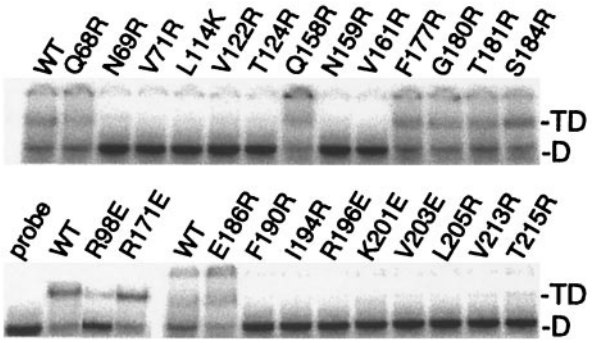


FIG. 6. Interaction of TATA DNA with TBP mutants. His-tagged yeast TBP mutants (30 nM), as indicated above each panel, were incubated with radiolabeled TATA DNA (~2 nM) and subjected to an electrophoretic mobility shift assay. WT, wild type; D, migration of free DNA; TD, migration of the TBP-DNA complexes. Stronger binding was observed in the presence of TFIIA, although the trend among the mutants remained unchanged (data not shown).

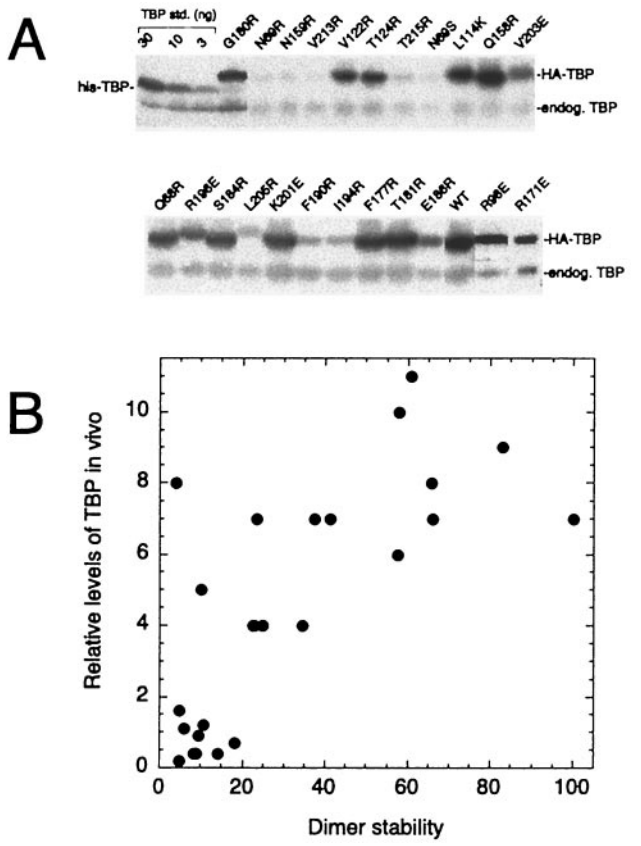


FIG. 7. In vivo steady-state level of TBP mutants correlates with dimer stability. (A) Yeast cells (YPH252) harboring pCALF-T(xxx-)(*PGK*) were grown in CSM-Leu plus 2% glucose liquid medium to an $OD_{600}$ of near 1. Equivalent numbers of cells (~0.5 ml) were then collected and subjected to SDS-PAGE and immunoblotting (ECL) with TBP antibodies. Purified recombinant TBP standards (std.), spiked into samples expressing a null version of HA-TBP, are shown. endog. TBP, endogenous wild-type TBP. Mutants not shown here are presented in reference 45. WT, wild type. (B) HA-TBP expression levels as a function of in vitro dimer stability. Data are from Table 1. The TBP expression levels are relative to that of endogenous TBP (set at 1.0), which is present at ~17,000 molecules per cell (45).

pressed. TBP(181C) had little effect (1.5-fold) on repressed levels of *lacZ* expression (data not shown). Since the conserved core of TBP is nevertheless functional in yeast (29, 85), it is therefore unlikely that TBP's nonconserved amino-terminal domain is a major inhibitor of TBP at this promoter.

The TAF1 TAND domain cannot account for the entirety of the inhibitory activity along TBP's concave surface, since mutations along this surface cause widespread derepression in a *taf1*(Δ*TAND*) strain, and deletion of the TAND domain by itself has little effect (24). Consistent with this, deletion of the TAND domain caused only a modest level of *lacZ* derepression (1.5-fold) (data not shown).

**Mutations along TBP's concave surface affect a different set of genes than that in a Mot1-defective TBP mutant.** Mot1 interacts with the concave surface of TBP (71), in addition to interacting with helix 2 of TBP's convex surface (6). To address whether the transcriptional derepression caused by mutations along TBP's concave surface might be due to a loss of functional interactions with Mot1 (or other negative regulators that target helix 2), we compared genome-wide gene expression patterns of cells expressing TBP that has been mutated along its concave surface with that of cells expressing a TBP mutant that is defective for Mot1 interactions. The K145E mutation lies along helix 2 of TBP's convex surface, and is defective for interactions with at least Mot1 and TFIIA in vitro (6, 21). The phenotype associated with the K145E mutation is suppressed by Mot1 overexpression but not by TFIIA overexpression, suggesting that it is primarily defective in Mot1 interactions in vivo (21). Recently, we reported the genome-wide expression pattern caused by mutations along TBP's concave surface (24). The study revealed that there are at least two distinct primary inhibitory interactions along TBP's concave surface, as well as a weaker secondary inhibitory interaction attributed to the TAF1 TAND domain. If K145E and mutations along the concave surface of TBP (such as V161R or V71R) affect the same interactions, they should generate similar genome-wide gene expression patterns.

The genome-wide expression pattern caused by TBP(K145E) was determined under conditions previously used to analyze mutations along TBP's concave surface (24). This included a brief (45-min) induction of TBP(K145E) under control of the *GAL10* promoter in cells harboring a wild-type copy of the *TBP* gene. This short exposure of cells to the TBP mutants attempts to minimize indirect effects. mRNA levels were compared to those in a reference sample in which a null mutant of TBP was induced. The K145E mutation led to significantly increased expression of 27 out of 4,988 genes, while 8 genes significantly decreased in expression. Mutations along TBP's concave surface have a much broader impact on genome-wide expression, with 374 genes being significantly affected in the V161R mutant (24). These genome-wide response patterns are robust in that distinct mutations along the concave surface of TBP give nearly identical changes in gene expression (Fig. 9, compare V71R and V161R).

Only 7 of the 35 genes significantly affected by the K145E mutation were also similarly affected by mutations along the concave surface of TBP. This low level of overlap and the minimal impact on genome-wide expression of K145E com-

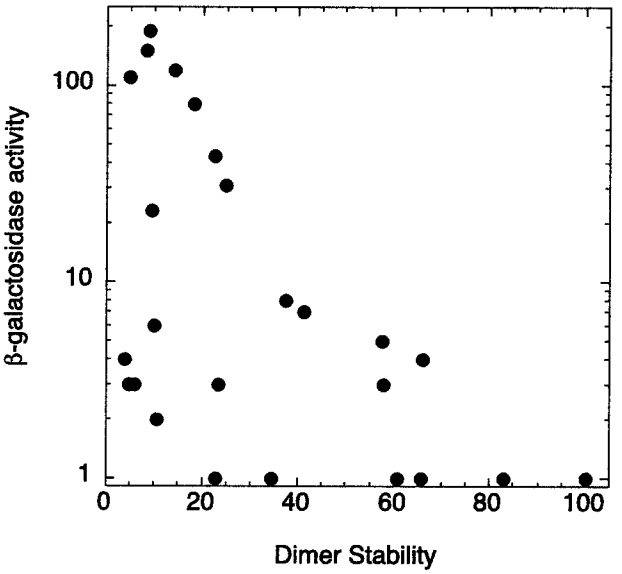


FIG. 8. Transcriptional repression correlates with TBP dimer stability. The experimental setup is the same as for Fig. 7, except cells also contained pADH1-lacZ and were grown in CSM-Leu-Ura plus 2% glucose liquid medium. β-Galactosidase activity is plotted on a $\log_{10}$ scale as a function of dimer stability.

pared to mutations along TBP's concave surface suggests that the interactions compromised by mutations along TBP's concave surface are distinct from the interactions compromised by K145E. Mot1, therefore, might not be the predominant inhibitor of TBP's concave surface.

It is possible that the minimal impact of K145E is due to potential defects in both negative (Mot1) and positive (TFIIA) interactions that render the mutant generally nonfunctional. If so, then the K145E mutation should nullify the effects of V161R and display an overall pattern that is similar to that of K145E. To test this, a K145E V161R double mutant was constructed and its impact on genome-wide expression was examined. As shown in Fig. 9, this double mutation caused widespread changes in gene expression that were similar to but distinct from those caused by the V161R mutation and clearly different from those caused by the K145E mutation. Therefore, K145E was not generally debilitating to TBP.

**Mutations along TBP's concave surface are partially toxic to cell growth.** Previously we showed that mutations along TBP's concave surface have a dominant slow-growth phenotype (24). To examine whether the present collection of mutants behave similarly, YPH252 was transformed with each of the mutants and growth rates in liquid medium and on solid medium were measured. As shown in Fig. 10 and summarized in Table 1 and Fig. 4A, the two methods gave similar results. Mutations along TBP's concave surface were partially toxic to cell growth. As demonstrated previously (24), this toxicity might be due to widespread misexpression of genes. With one exception, all mutants that displayed partial toxicity failed to support cell growth in the absence of wild-type TBP. R196E stood out as causing slow growth regardless of the presence of wild-type TBP and thus might reflect altered interactions that are distinctly different from those along TBP's concave surface.

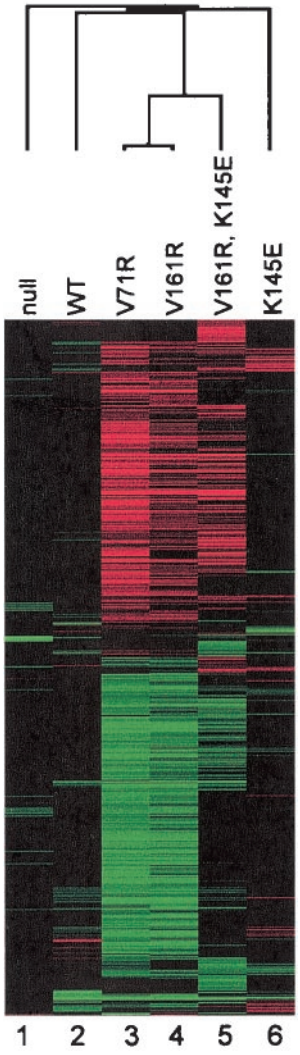


FIG. 9. Cluster analysis of genome-wide expression patterns of TBP mutants. Cluster and Treeview (33) were used to cluster significant changes in gene expression for 811 genes that changed significantly in at least one experiment, using the criteria in reference 24. Each row corresponds to a particular gene, whose expression level is being measured relative to a reference state (an isogenic strain that briefly expresses the TBP null mutant [24]). Each column corresponds to a particular TBP mutant. The color intensities correspond to fold increases (red) or decreases (green) in gene expression. Black and gray correspond to no changes in gene expression, with gray generally indicating that the gene was not expressed in either the reference or test sample. Both the rows and columns were clustered using a hierarchical algorithm. The dendrogram for column clustering is shown. Data from columns 2 to 4 are from reference 24.

**TBP mutants display synthetic toxicity in combination with ΔTAND.** Cells lacking the TAF1 TAND domain have a mild growth defect, which can be suppressed by TBP overexpression (10, 24, 54). Mutations along TBP's concave surface cause synthetic toxicity in combination with ΔTAND (51), and this can occur in a wild-type TBP background (24). To examine whether this dominant synthetic toxicity exists with mutations throughout the crystallographic dimer interface, we employed the *TAF1* shuffle strain Y13.2. This strain has a deletion of the

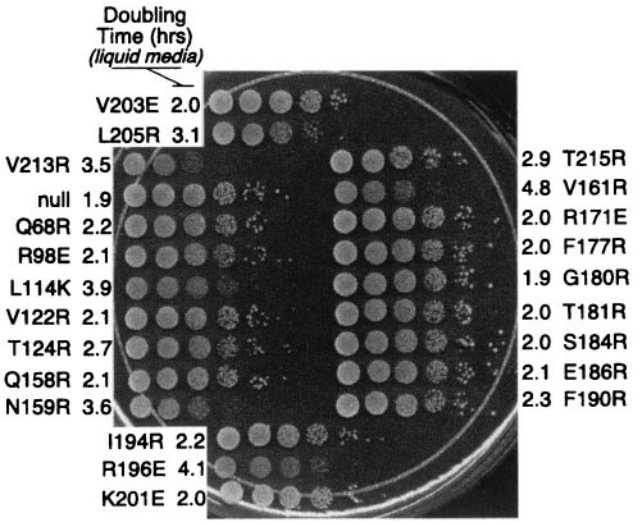


FIG. 10. Cell growth toxicity imparted by TBP mutants. Strain YPH252 (wild type for TBP) was transformed with a plasmid harboring a gene coding for wild-type HA-tagged TBP or the indicated mutant expressed under the control of the highly active *PGK1* promoter. Cell doubling times in liquid medium (CSM-Leu plus 2% glucose) were calculated and are reported next to each mutant. An equivalent number of cells were then serially diluted 10-fold, spotted onto solid medium (CSM-Leu plus 2% glucose), and incubated at 30°C for 3 days.

chromosomal *TAF1* gene and harbors *TAF1* on a Ura-marked plasmid (*TAF1*/Ura). From Y13.2, two strains that additionally contained either *TAF1*/Trp or *taf1*(Δ*TAND*)/Trp plasmids were constructed. The intent was to transform the *TBP* mutants into each of these strains, shuffle out *TAF1*/Ura, and assay growth rates. However, due to the intrinsic partial toxicity of some of the TBP mutants, propagation of the shuffle strain harboring these mutants tended to select for faster-growing revertants that gave high background on the 5-FOA selection plates. Therefore, we chose an alternative approach in which growth was examined immediately upon transformation of the final test strains. To do this, we constructed two additional strains in which the *TAF1*/Ura plasmid was replaced with an empty vector (pRS416/Ura). The resulting four strains allowed us to measure, in parallel, toxicity in the presence of (i) one copy of *TAF1*, (ii) two copies of *TAF1*, (iii) one copy of *taf1*(Δ*TAND*), and (iv) one copy of *TAF1* plus one copy of *taf1*(Δ*TAND*). Each of the four strains was transformed with the TBP mutants and immediately serially diluted and plated on selective medium at 23, 30, and 37°C. The data for 37°C are shown in Fig. 11 and summarized in Table 1 and Fig. 4A.

All TBP mutants efficiently transformed the *TAF1*, *TAF1*/*TAF1*, and *taf1*(Δ*TAND*)/*TAF1* strains. For a particular TBP mutant, each of the *TAF1* strains grew at similar rates that were characteristic of the partial toxicity, if any, imparted by each TBP mutant. TBP mutants that were not toxic efficiently transformed the *taf1*(Δ*TAND*) strain. However, TBP mutants that displayed partial toxicity in the presence of wild-type *TAF1* (Fig. 10) generally displayed synthetic toxicity in combination with ΔTAND (Fig. 11; summarized in Table 1 and Fig. 4A). The most severe were N69R, V71R, N159R, and V161R, which showed no growth after 4 days. V122R, T124R, V213R,

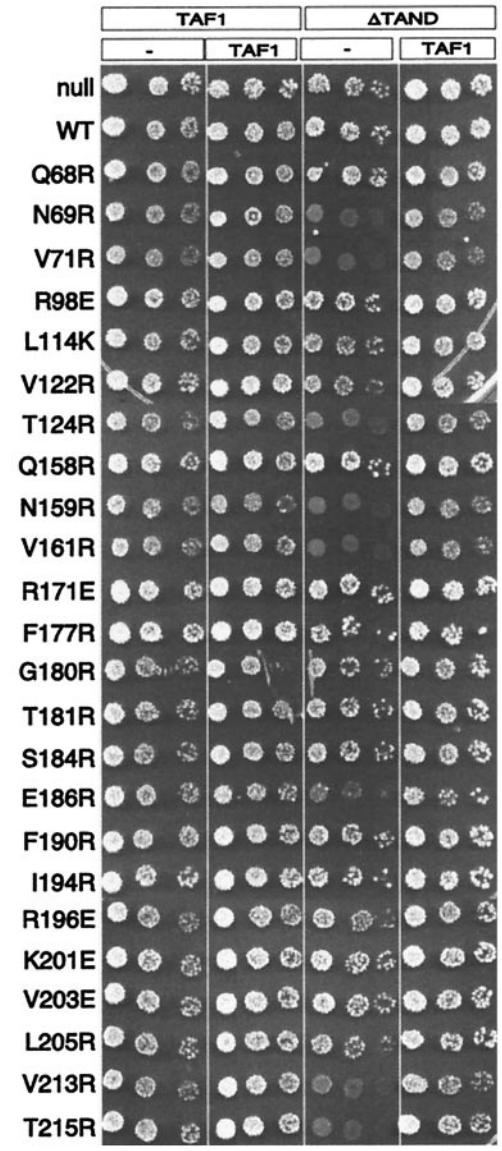


FIG. 11. TBP mutants display synthetic toxicity with ΔTAND. Plasmids harboring the mutant TBPs were transformed into the *taf1*Δ strain Y13.2 that contained either wild-type *TAF1* or *taf1*(Δ*TAND*) on a Trp-marked plasmid and either a null (pRS416) or *TAF1* on a Ura-marked plasmids. Cells were immediately serially diluted fivefold dilution, spotted onto solid medium (CSM-Ura-Trp-Leu), and incubated at 37°C for 3 days. Similar results were obtained at 23 and 30°C. WT, wild type.

and T215R were also severe and displayed very weak growth after 4 days. These eight mutants also caused the most transcriptional derepression (Table 1), which suggests that the synthetic toxicity is due to a combined loss of inhibitory activity from TAND and the concave surface of TBP. R196E and L114K, which both showed relatively high levels of toxicity in the presence of wild-type *TAF1* (Fig. 10), did not display synthetic toxicity with ΔTAND. Therefore, their toxicity might be unrelated to the toxicity displayed by the other mutants. Interestingly, E186R displayed synthetic toxicity but was otherwise not toxic and did not cause transcriptional derepression. As

E186 interacts with TFIIB, we suspect that the E186R synthetic toxicity reflects a mechanism that is distinct from that of the others. In general, the synthetic toxicity, while dominant to wild-type *TBP*, was recessive to wild-type *TAF1*.

## DISCUSSION

TBP's concave surface interacts with multiple factors, which include DNA, the TAND domain of TAF1, Mot1, and a second molecule of TBP to form a dimer. Here, we have mapped three of these interactions by creating 24 point mutations throughout TBP's crystallographic dimer interface. The in vitro and in vivo properties of these mutants are summarized in Fig. 4. The data for all three interactions are in general agreement with the NMR-crystallographic structures of these or related complexes.

The majority of the mutants have similar phenotypes in vivo. About half do not support cell viability when provided as the sole source of TBP, while several others support weak growth. When the TBP mutants were expressed in a wild-type TBP strain, their steady-state levels correlated with dimer stability. A similar correlation was observed for a subset of the mutants examined in a *taf1*(Δ*TAND*) strain, indicating that defects in TAND interactions were not responsible (24). Six TBP mutants that were severely defective in DNA binding in vitro were present at high steady-state levels in vivo, which suggests that defects in DNA binding were not responsible for the increased turnover of the TBP mutants. These results provide further support for our previous suggestion that dimerization protects TBP from degradation in vivo (45).

A set of eight mutations that cluster at the center of TBP's cavity caused high levels of transcriptional derepression. Additional mutations surrounding this cluster caused modest derepression. The amount of derepression in vivo correlated with dimer instability measured in vitro. In general, the more severe dimerization mutants were partially toxic to cell growth and displayed synthetic toxicity in combination with ΔTAND. Taken together, these data define a major inhibitory patch along TBP's concave surface. This region is distinct from a previously defined NC2 inhibitory surface on TBP's convex surface (21). Genome-wide expression profiling, presented here and elsewhere (24), indicates that the TAF1 TAND domain and Mot1 are unlikely to be the primary inhibitors targeting TBP's concave surface. These factors might make minor contributions. As presented in more detail below, other potential inhibitory mechanisms cannot readily account for the inhibition of TBP's concave surface. However, the data are fully consistent with a model in which TBP is prevented from binding to accessible promoters by homodimerization. TBP recruitment to promoters, which is important for transcription complex assembly, would require dimers to dissociate into monomers.

**Potential alternative sources of inhibition along TBP's concave surface.** TBP might be inhibited by a number of factors, including the TAF1 TAND domain, Mot1, NC2, Spt3/Spt8, the Ccr4-Not complex, TBP's amino terminal domain, and TBP homodimerization. Alternatively, TBP could be sequestered at nonpromoter chromosomal sites through direct contact with DNA. The transcriptional derepression caused by mutations along TBP's concave surface could in principle arise from defects in one or more of these interactions. It is also possible that the mutations create novel positive interactions that lead to derepression. Below, we discuss each of these possibilities in light of the available evidence.

The TAF1 TAND I domain interacts with the concave surface of TBP and inhibits TATA binding in vitro (11, 24, 52, 53, 70). Therefore, transcriptional derepression observed with mutations along TBP's concave surface could be due to a loss of TAND interactions. However, several observations indicate that TAND is not the primary inhibitor. (i) Deletion of the TAND domain does not lead to derepression of the promoter used in this study and has little impact genome wide (24). (ii) Transcriptional derepression caused by mutations along TBP's concave surface is unabated in a strain with the TAND domain deleted, indicating that TAND is not required for transcriptional derepression. However, deletion of TAND enhances the level of derepression observed with the TBP mutants (24). (iii) Despite the observation that mutations along TBP's concave surface impair TAND binding, many of the same mutations do not cause defects in binding full-length TAF1 in yeast crude extracts (24). These findings indicate that the transcriptional derepression arising from mutations along TBP's concave surface is not caused solely or predominantly by a loss of TAND interactions. TAND does play an inhibitory role, but it appears to be secondary to another inhibitor.

Mot1 uses the energy of ATP hydrolysis to dissociate TBP-DNA complexes (7, 8, 23). Mot1 and TFIIA interact with helix 2 on TBP's convex surface (1, 6, 18, 21, 59). The K145E mutation on helix 2 eliminates binding (21). In vivo, phenotypes associated with K145E are suppressed by Mot1 overexpression but not by TFIIA overexpression, which suggests that K145E is primarily defective in Mot1 interactions (21). Mot1 might also interact with TBP's concave surface (71). Therefore, it is plausible that the transcriptional derepression caused by mutations along TBP's concave surface is due to defects in Mot1 interactions. A number of observations render this possibility unlikely. First, mutations along TBP's concave surface do not show defects in Mot1 binding in coimmunoprecipitation assays from yeast whole-cell extracts (supplement to reference 24). Second, genome-wide expression analysis reveals that genes that increase in expression with K145E are largely distinct from those caused by mutations along TBP's concave surface. In addition, the genome-wide expression pattern of a helix 2 concave-surface double mutant (K145E V161R) was approximately additive to the effects of the single mutants. The general lack of overlapping effects of the individual mutants and the additive effects of the double mutant suggest that the two surfaces primarily affect different processes.

It has been suggested that TBP is sequestered at high-affinity nonpromoter chromosomal sites in vivo and is liberated by Mot1 (28, 68). Since our experiments with the TBP mutants are performed in a *MOT1* strain, TBP should not be sequestered. However, if Mot1 is inefficient, then there might be competition between promoter and nonpromoter sites for TBP binding. Conceivably, mutations along the concave DNA binding surface of TBP could elicit the same effect as Mot1 by selectively destabilizing high-affinity nonproductive TBP-DNA complexes, allowing the mutants to assemble productively at promoters. Several observation are inconsistent with this possibility. First, chromatin immunoprecipitation studies indicate

that TBP is generally not bound to DNA outside highly active promoters (13, 56, 57, 64). Second, 30-fold overexpression of wild-type TBP (enough to cover one-third of all chromosomal DNA) does not cause any growth defects or affect global gene expression patterns (7, 24, 45, 74, 76). If a limiting amount of TBP were sequestered at high-affinity nonpromoter sites, then increased levels of TBP should lead to a widespread increase in gene expression. Third, wild-type TBP overexpression in the context of the TBP mutants should exacerbate the mutant phenotypes, since wild-type TBP would preferentially bind nonpromoter sites, making the mutants more available. This was not observed; instead, wild-type TBP partially suppresses the mutants (45). Fourth, several mutants that are severely impaired in DNA binding (F190R, I194R, R196E, K201E, and L205R) cause only a modest increase in transcription (<5-fold increase in β-galactosidase activity, compared to 100- to 200-fold for others). Fifth, a TBP mutant (V161E) causes primarily an increase in transcription when examined on a genome-wide scale, while another mutant (F182V) causes primarily a decrease in transcription (24). Their selective and opposing behaviors indicate that promoter competition is unlikely, where any increase in transcription of one set of genes must causally come at the expense of decreased expression of another set of genes. Taken together, these observations suggest that the transcriptional derepression caused by mutations along TBP's concave surface is not due to their selective release from an inactive chromosomally bound pool.

NC2 is an inhibitor of TBP and acts primarily on TBP-TATA complexes by preventing the subsequent loading of TFIIA and TFIIB (21, 38, 49, 67). NC2 interacts primarily with the C-terminal convex surface of TBP (21, 46). A brief exposure of yeast cells to the NC2 interaction-defective mutant TBP(F182V) leads to a further increase in expression of many highly expressed genes, which is consistent with an inhibitory role for NC2 at these genes (24). In contrast, mutations along TBP's concave surface lead to decreased expression of the same set of F182V-sensitive genes, which might be due to loss of positive interactions with promoter DNA (24). At a different set of genes, mutations along TBP's concave surface lead to increased expression. These genes are generally unaffected by the F182V mutation (24). Taken together, these observations indicate that the transcriptional derepression caused by mutations along TBP's concave surface is unlikely to be due to a loss of NC2-TBP interactions.

Spt3 and Spt8 are subunits of the SAGA chromatin-remodeling complex and play an important positive role in transcriptional activation (14, 32, 35, 39, 40, 58). However, Spt3 and Spt8 also inhibit TBP (12). Spt3 has genetic interactions with amino acids R171 and F177 (34). It is possible that Spt3 inhibits TBP function through direct interactions with the convex region of TBP defined in part by R171 and F177, although direct interactions have not been demonstrated. It is also plausible that Spt3 in conjunction with Spt8 inhibits TBP function through additional contacts with TBP's concave surface, although there is no evidence addressing this possibility. We have constructed mutations R171E and F177R as part of the series of mutations along TBP's crystallographic dimer interface. The R171E and F177R TBP mutants are generally functional, since they support growth, albeit slowly. An *spt3*Δ mutant also has a slow-growth phenotype (82). Neither R171E nor F177R causes transcriptional derepression of the reporter gene used in this study, indicating that the derepression caused by mutations along TBP's concave surface is unlikely to be due to defects in Spt3 interactions. Consistent with this conclusion, mutations along TBP's concave surface caused transcriptional derepression (albeit tempered) in an *spt3*Δ strain (data not shown). Thus, Spt3 does not appear to be a predominant inhibitor of TBP's concave surface at the reporter gene used in this study.

Ccr4-Not is a complex of several proteins implicated in negatively regulating TBP (9, 31, 66). Because mutations along TBP's concave surface generate phenotypes distinct from those caused by *not* mutations, it has been proposed that the Ccr4-Not complex does not inhibit through TBP's concave surface (9). Instead, the Ccr4-Not complex might regulate TBP through the TFIID TAF complex, possibly through functional interactions with TAF1 (9, 31).

TBP's amino-terminal domain inhibits TBP-TATA interactions in vitro (55). Deletion of this domain is not lethal but suppresses transcriptional activation defects along TBP's concave surface, which is consistent with the notion that the amino-terminal domain inhibits TBP-TATA interactions in vivo (60). To address whether the transcriptional derepression caused by mutations along TBP's concave surface is due to loss of inhibitory interactions with TBP's amino-terminal domain, we deleted its amino-terminal domain. No significant derepression was observed, indicating that TBP's amino-terminal domain does not contribute predominantly to TBP inhibition at the reporter gene used in this study.

It is possible that mutations along TBP's concave surface relax or alter its specificity for the TATA box, thereby allowing the mutants to recognize a wider variety of sequences (3, 5, 79). There is a precise correspondence between a TATA DNA sequence and its binding location along TBP's concave surface (3, 48, 50). If broadened DNA specificity were the primary basis for the phenotypes of our mutants, different TBP mutations would be expected to give rise to distinct ranges of specificity and thus generate a largely nonoverlapping pattern of transcriptional derepression in genome-wide expression studies. However, mutations at a variety of locations on TBP's concave surface, and chemically distinct mutations at the same locations, give rise to very similar patterns of transcriptional derepression throughout the yeast genome (24).

Mutations along TBP's concave surface that increase transcription from promoters repressed by Cyc8-Tup1 or Sin3-Rpd3 were isolated (36). It was proposed that these mutations create an unusual TBP structure that allows them to preferentially access TATA elements in chromatin templates (36). Although we cannot exclude this possibility for our collection of mutants, it would seem unlikely that chemically different mutations at a large number and variety of amino acid side chains can introduce the same structural change in TBP to produce a novel function which can act on hundreds of genes throughout the genome. A more parsimonious explanation is that such mutations prevent an inhibitor from associating with TBP, thereby unmasking a latent function, such as TATA binding.

**TBP dimerization as a predominant autoinhibitory state of TBP in vivo.** A number of observation support the notion that TBP self-associates, thereby inhibiting DNA binding and transcription complex assembly. First, TBP crystallizes as a dimer

in which the DNA binding and dimerization interfaces overlap (22, 69). Second, analytical ultracentrifugation (20, 30), fluorescence anisotropy (72), gel filtration (26, 47), glycerol gradients (42, 47), chemical cross-linking (26, 36, 42, 44, 45), and DNA binding kinetics (25) show that TBP specifically self-associates in vitro. Third, several experiments involving chemical cross-linking, gel filtration, and pulldown assays indicate that TFIID dimerizes (81). Fourth, TFIIA, which plays a multifunctional role in removing TBP-targeted inhibitors, specifically accelerates dimer dissociation and DNA binding of TBP-TFIID (27). Fifth, TBP can be cross-linked into dimers inside human tissue culture cells and in yeast cells (45, 81). Sixth, mutations along TBP's crystallographic dimer interface inhibit TBP dimerization and lead to transcription derepression in vivo (24, 45; this study). Taken together, these findings suggest that TBP-TFIID homodimerization plays an important autoinhibitory role in vivo.

The notion that TBP dimerizes in vivo has been controversial. Since yeast TBP dimerizes in vitro with low affinity (20) and since coimmunoprecipitation (20, 78) and electron microscopy (2, 16, 62) studies have failed to detect TFIID dimers, the physiological relevance of this interaction has been questioned. From the available evidence, we surmise that yeast TBP, in general, forms weak dimers (and higher-order structures) in vitro, whereas human TBP forms stronger dimers. Conditions used to purify and/or prepare TFIID for electron microscopy might favor a more monomeric configuration. As noted in one study on TBP self-association, solution and handling conditions may dictate whether monomers or multimers prevail (72). Since in vitro conditions cannot fully recapitulate the hierarchy of competing protein-protein interactions and their affinities as they exist within a living cell, it might be erroneous to conclude anything about the propensity for TBP to dimerize or not dimerize in vivo based solely on the magnitude of an in vitro-determined $K_D$ value.

Of the 24 amino acids targeted for mutagenesis in this study, eight mutations (N69R, V71R, V122R, T124R, N159R, V161R, V213R, and T215R) stand out as causing extraordinarily high levels of transcriptional derepression. These eight amino acids form a continuous surface along the deepest part of TBP's concave surface. Virtually all are buried in the crystallographic dimer and are invariant from yeast to humans. Consistent with these properties, mutation of any of these amino acids to arginine destabilizes dimer formation in vitro. These mutations also destabilize TATA binding and so might be unable to achieve their full derepression potential in vivo. Studies by Geisberg and Struhl with a similar set of mutants suggest that these mutants nevertheless bind promoter DNA in vivo (36).

A second set of mutants (Q68R, L114K, Q158R, S184R, F190R, I194R, R196E, K201E, V203E, and L205R) show intermediate levels of transcriptional derepression. These amino acids are also identical in yeast and humans. Consistent with their intermediate transcriptional output, several show intermediate levels of dimer stability and reside near the solvent-exposed periphery of the crystallographic dimer interface. Three of these mutants (F190R, R196E, and L205R) are buried deep within the interface and are highly defective for dimerization. We suspect that their intermediate behavior is due to relatively greater defects in essential positive interactions, such as DNA binding, compared to the mutants described above.

Mutation of the three nonconserved amino acids F177, G180, and T181 had little effect on dimerization and caused little derepression. These amino acids are not constrained in the dimer crystal structure. R98E and R171E appeared to be partially defective for dimerization. However, the crystal structure suggests that these mutations might enhance dimer stability. The pulldown assay, used to measured dimerization, is a competition between homodimers present in solution and heterodimers formed on the resin. If homodimer mutants are more stable and exchange onto the resin more slowly, fewer of these mutants would be retained on the resin. E186 resides along the TFIIB interface, and so mutation of this amino acid is expected to render TBP largely inactive for transcription. Interestingly, this mutation displays dominant synthetic toxicity in combination with deletion of the TAND domain. The basis for this is not known, although a TBP(E186R)-TATA complex might impair transcription complex assembly. TAND might function in this regard to assist in removing nonproductive TBP from DNA.

**Yeast and *Drosophila* TAF1 TAND I domains have similar interfaces with TBP.** Yeast TAND is about half the size of *Drosophila* TAND and is poorly conserved. It was therefore surprising to find that yeast TAND contacts nearly the same surface along TBP as *Drosophila* TAND I. Of the 67 amino acids present in the *Drosophila* TAND I NMR structure (65), ~50 amino acids reside within the concave surface of TBP. Therefore, we expect the yeast TAND I domain to be minimally 50 amino acids in size. The yeast TAND I domain, however, has been demarcated at ~28 amino acids (52, 54). Moreover, yeast TAND I is only ~10 amino acids away from TAND II, which is believed to interact with helix 2 of TBP's convex surface (52). Based on these facts, it is not clear how yeast TAND I can occupy the same region as *Drosophila* TAND I yet still provide a sufficient linker to allow TAND II to bind helix 2 of TBP. One plausible explanation is that helix 3 of *Drosophila* TAND I is not present in yeast TAND I (Fig. 4B). This would allow the polypeptide chain to leave TBP's concave surface early and provide a sufficient linker for TAND II. In support of this possibility, the TBP amino acids Q158 and K201, which make contact with *Drosophila* TAND I helix 3, have no effect on yeast TAND binding when mutated. Also consistent with a smaller binding surface, yeast TAND I has a weaker affinity for TBP than *Drosophila* TAND I (54).

## ACKNOWLEDGMENTS

We thank Lata Chitikila, Diane Alexander, and Kevin Halbe for technical assistance and members of the Pugh laboratory for helpful discussions.

This work was supported by NIH grant GM59055.

## REFERENCES

1. **Adamkewicz, J. I., K. E. Hansen, W. A. Prud'homme, J. L. Davis, and J. Thorner.** 2001. High affinity interaction of yeast transcriptional regulator, Mot1, with TATA box-binding protein (TBP). J. Biol. Chem. **276:**11883–11894.
2. **Andel, F., III, A. G. Ladurner, C. Inouye, R. Tjian, and E. Nogales.** 1999. Three-dimensional structure of the human TFIID-IIA-IIB complex. Science **286:**2153–2156.
3. **Arndt, K. M., S. L. Ricupero, D. M. Eisenmann, and F. Winston.** 1992. Biochemical and genetic characterization of a yeast TFIID mutant that alters transcription in vivo and DNA binding in vitro. Mol. Cell. Biol. **12:**2372–2382.

4. **Arndt, K. M., S. Ricupero-Hovasse, and F. Winston.** 1995. TBP mutants defective in activated transcription in vivo. EMBO J. **14:**1490–1497.
5. **Arndt, K. M., C. R. Wobbe, S. Ricupero-Hovasse, K. Struhl, and F. Winston.** 1994. Equivalent mutations in the two repeats of yeast TATA-binding protein confer distinct TATA recognition specificities. Mol. Cell. Biol. **14:**3719–3728.
6. **Auble, D. T., and S. Hahn.** 1993. An ATP-dependent inhibitor of TBP binding to DNA. Genes Dev. **7:**844–856.
7. **Auble, D. T., K. E. Hansen, C. G. Mueller, W. S. Lane, J. Thorner, and S. Hahn.** 1994. Mot1, a global repressor of RNA polymerase II transcription, inhibits TBP binding to DNA by an ATP-dependent mechanism. Genes Dev. **8:**1920–1934.
8. **Auble, D. T., D. Wang, K. W. Post, and S. Hahn.** 1997. Molecular analysis of the SNF2/SWI2 protein family member MOT1, an ATP-driven enzyme that dissociates TATA-binding protein from DNA. Mol. Cell. Biol. **17:**4842–4851.
9. **Badarinarayana, V., Y. C. Chiang, and C. L. Denis.** 2000. Functional interaction of CCR4-NOT proteins with TATAA-binding protein (TBP) and its associated factors in yeast. Genetics **155:**1045–1054.
10. **Bai, Y., G. M. Perez, J. M. Beechem, and P. A. Weil.** 1997. Structure-function analysis of TAF130: identification and characterization of a high-affinity TATA-binding protein interaction domain in the N terminus of yeast TAF(II)130. Mol. Cell. Biol. **17:**3081–3093.
11. **Banik, U., J. M. Beechem, E. Klebanow, S. Schroeder, and P. A. Weil.** 2001. Fluorescence-based analyses of the effects of full-length recombinant TAF130p on the interaction of TATA box-binding protein with TATA box DNA. J. Biol. Chem. **276:**49100–49109.
12. **Belotserkovskaya, R., D. E. Sterner, M. Deng, M. H. Sayre, P. M. Lieberman, and S. L. Berger.** 2000. Inhibition of TATA-binding protein function by SAGA subunits Spt3 and Spt8 at Gcn4-activated promoters. Mol. Cell. Biol. **20:**634–647.
13. **Bhaumik, S. R., and M. R. Green.** 2002. Differential requirement of SAGA components for recruitment of TATA-box-binding protein to promoters in vivo. Mol. Cell. Biol. **22:**7365–7371.
14. **Bhaumik, S. R., and M. R. Green.** 2001. SAGA is an essential in vivo target of the yeast acidic activator Gal4p. Genes Dev. **15:**1935–1945.
15. **Blair, W. S., and B. R. Cullen.** 1997. A yeast TATA-binding protein mutant that selectively enhances gene expression from weak RNA polymerase II promoters. Mol. Cell. Biol. **17:**2888–2896.
16. **Brand, M., C. Leurent, V. Mallouh, L. Tora, and P. Schultz.** 1999. Three-dimensional structures of the TAFII-containing complexes TFIID and TFTC. Science **286:**2151–2153.
17. **Bryant, G. O., L. S. Martel, S. K. Burley, and A. J. Berk.** 1996. Radical mutations reveal TATA-box binding protein surfaces required for activated transcription in vivo. Genes Dev. **10:**2491–2504.
18. **Buratowski, S., and H. Zhou.** 1992. Transcription factor IID mutants defective for interaction with transcription factor IIA. Science **255:**1130–1132.
19. **Burley, S. K., and R. G. Roeder.** 1996. Biochemistry and structural biology of transcription factor IID (TFIID). Annu. Rev. Biochem. **65:**769–799.
20. **Campbell, K. M., R. T. Ranallo, L. A. Stargell, and K. J. Lumb.** 2000. Reevaluation of transcriptional regulation by TATA-binding protein oligomerization: predominance of monomers. Biochemistry **39:**2633–2638.
21. **Cang, Y., D. T. Auble, and G. Prelich.** 1999. A new regulatory domain on the TATA-binding protein. EMBO J. **18:**6662–6671.
22. **Chasman, D. I., K. M. Flaherty, P. A. Sharp, and R. D. Kornberg.** 1993. Crystal structure of yeast TATA-binding protein and model for interaction with DNA. Proc. Natl. Acad. Sci. USA **90:**8174–8178.
23. **Chicca, J. J., II, D. T. Auble, and B. F. Pugh.** 1998. Cloning and biochemical characterization of TAF-172, a human homolog of yeast Mot1. Mol. Cell. Biol. **18:**1701–1710.
24. **Chitikila, C., K. L. Huisinga, J. D. Irvin, M. Mitra, and B. F. Pugh.** 2002. Interplay of TBP inhibitors in global transcriptional control. Mol. Cell **10:**871–882.
25. **Coleman, R. A., and B. F. Pugh.** 1997. Slow dimer dissociation of the TATA binding protein dictates the kinetics of DNA binding. Proc. Natl. Acad. Sci. USA **94:**7221–7226.
26. **Coleman, R. A., A. K. Taggart, L. R. Benjamin, and B. F. Pugh.** 1995. Dimerization of the TATA binding protein. J. Biol. Chem. **270:**13842–13849.
27. **Coleman, R. A., A. K. P. Taggart, S. Burma, J. J. Chicca, I. I., and B. F. Pugh.** 1999. TFIIA regulates TBP and TFIID dimers. Mol. Cell **4:**451–457.
28. **Collart, M. A.** 1996. The *NOT*, *SPT3*, and *MOT1* genes functionally interact to regulate transcription at core promoters. Mol. Cell. Biol. **16:**6668–6676.
29. **Cormack, B. P., M. Strubin, A. S. Ponticelli, and K. Struhl.** 1991. Functional differences between yeast and human TFIID are localized to the highly conserved region. Cell **65:**341–348.
30. **Daugherty, M. A., M. Brenowitz, and M. G. Fried.** 1999. The TATA-binding protein from Saccharomyces cerevisiae oligomerizes in solution at micromolar concentrations to form tetramers and octamers. J. Mol. Biol. **285:**1389–1399.
31. **Deluen, C., N. James, L. Maillet, M. Molinete, G. Theiler, M. Lemaire, N. Paquet, and M. A. Collart.** 2002. The Ccr4-Not complex and yTAF1 [yTaf(II)130p/yTaf(II)145p] show physical and functional interactions. Mol. Cell. Biol. **22:**6735–6749.
32. **Dudley, A. M., C. Rougeulle, and F. Winston.** 1999. The Spt components of SAGA facilitate TBP binding to a promoter at a post-activator-binding step in vivo. Genes Dev. **13:**2940–2945.
33. **Eisen, M. B., P. T. Spellman, P. O. Brown, and D. Botstein.** 1998. Cluster analysis and display of genome-wide expression patterns. Proc. Natl. Acad. Sci. USA **95:**14863–14868.
34. **Eisenmann, D. M., K. M. Arndt, S. L. Ricupero, J. W. Rooney, and F. Winston.** 1992. SPT3 interacts with TFIID to allow normal transcription in Saccharomyces cerevisiae. Genes Dev. **6:**1319–1331.
35. **Eisenmann, D. M., C. Chapon, S. M. Roberts, C. Dollard, and F. Winston.** 1994. The Saccharomyces cerevisiae SPT8 gene encodes a very acidic protein that is functionally related to SPT3 and TATA-binding protein. Genetics **137:**647–657.
36. **Geisberg, J. V., and K. Struhl.** 2000. TATA-binding protein mutants that increase transcription from enhancerless and repressed promoters in vivo. Mol. Cell. Biol. **20:**1478–1488.
37. **Gietz, R. D., and R. H. Schiestl.** 1995. Transforming yeast with DNA. Methods Mol. Biol. Cell. Biol. **5:**255–269.
38. **Goppelt, A., and M. Meisterernst.** 1996. Characterization of the basal inhibitor of class II transcription NC2 from *Saccharomyces cerevisiae*. Nucleic Acids Res. **24:**4450–4455.
39. **Grant, P. A., L. Duggan, J. Cote, S. M. Roberts, J. E. Brownell, R. Candau, R. Ohba, T. Owen-Hughes, C. D. Allis, F. Winston, S. L. Berger, and J. L. Workman.** 1997. Yeast Gcn5 functions in two multisubunit complexes to acetylate nucleosomal histones: characterization of an Ada complex and the SAGA (Spt/Ada) complex. Genes Dev. **11:**1640–1650.
40. **Grant, P. A., D. Schieltz, M. G. Pray-Grant, D. J. Steger, J. C. Reese, J. R. Yates III, and J. L. Workman.** 1998. A subset of TAF(II)s are integral components of the SAGA complex required for nucleosome acetylation and transcriptional stimulation. Cell **94:**45–53.
41. **Hagemeier, C., S. Walker, R. Caswell, T. Kouzarides, and J. Sinclair.** 1992. The human cytomegalovirus 80-kilodalton but not the 72-kilodalton immediate-early protein transactivates heterologous promoters in a TATA box-dependent mechanism and interacts directly with TFIID. J. Virol. **66:**4452–4456.
42. **Icard-Liepkalns, C.** 1993. Binding activity of the human transcription factor TFIID. Biochem. Biophys. Res. Commun. **193:**453–459.
43. **Imbalzano, A. N., H. Kwon, M. R. Green, and R. E. Kingston.** 1994. Facilitated binding of TATA-binding protein to nucleosomal DNA. Nature **370:**481–485.
44. **Jackson-Fisher, A. J., S. Burma, M. Portnoy, L. Schneeweis, R. A. Coleman, M. Mitra, C. Chitikila, and B. F. Pugh.** 1999. Dimer dissociation and thermosensitivity kinetics of the *Saccharomyces cerevisiae* and human TATA binding proteins. Biochemistry **38:**11340–11348.
45. **Jackson-Fisher, A. J., C. Chitikila, M. Mitra, and B. F. Pugh.** 1999. A role for TBP dimerization in preventing unregulated gene expression. Mol. Cell **3:**717–727.
46. **Kamada, K., F. Shu, H. Chen, S. Malik, G. Stelzer, R. G. Roeder, M. Meisterernst, and S. K. Burley.** 2001. Crystal structure of negative cofactor 2 recognizing the TBP-DNA transcription complex. Cell **106:**71–81.
47. **Kato, K., Y. Makino, T. Kishimoto, J. Yamauchi, S. Kato, M. Muramatsu, and T. Tamura.** 1994. Multimerization of the mouse TATA-binding protein (TBP) driven by its C-terminal conserved domain. Nucleic Acids Res. **22:**1179–1185.
48. **Kim, J. L., D. B. Nikolov, and S. K. Burley.** 1993. Co-crystal structure of TBP recognizing the minor groove of a TATA element. Nature **365:**520–527.
49. **Kim, S., J. G. Na, M. Hampsey, and D. Reinberg.** 1997. The Dr1/DRAP1 heterodimer is a global repressor of transcription in vivo. Proc. Natl. Acad. Sci. USA **94:**820–825.
50. **Kim, Y., J. H. Geiger, S. Hahn, and P. B. Sigler.** 1993. Crystal structure of a yeast TBP/TATA-box complex. Nature **365:**512–520.
51. **Kobayashi, A., T. Miyake, Y. Ohyama, M. Kawaichi, and T. Kokubo.** 2001. Mutations in the TATA-binding protein, affecting transcriptional activation, show synthetic lethality with the TAF145 gene lacking the TAF N-terminal domain in Saccharomyces cerevisiae. J. Biol. Chem. **276:**395–405.
52. **Kokubo, T., M. J. Swanson, J. I. Nishikawa, A. G. Hinnebusch, and Y. Nakatani.** 1998. The yeast TAF145 inhibitory domain and TFIIA competitively bind to TATA-binding protein. Mol. Cell. Biol. **18:**1003–1012.
53. **Kotani, T., K. Banno, M. Ikura, A. G. Hinnebusch, Y. Nakatani, M. Kawaichi, and T. Kokubo.** 2000. A role of transcriptional activators as antirepressors for the autoinhibitory activity of TATA box binding of transcription factor IID. Proc. Natl. Acad. Sci. USA **97:**7178–7183.
54. **Kotani, T., T. Miyake, Y. Tsukihashi, A. G. Hinnebusch, Y. Nakatani, M. Kawaichi, and T. Kokubo.** 1998. Identification of highly conserved amino-terminal segments of dTAFII230 and yTAFII145 that are functionally interchangeable for inhibiting TBP-DNA interactions in vitro and in promoting yeast cell growth in vivo. J. Biol. Chem. **273:**32254–32264.
55. **Kuddus, R., and M. C. Schmidt.** 1993. Effect of the non-conserved N-terminus on the DNA binding activity of the yeast TATA binding protein. Nucleic Acids Res. **21:**1789–1796.
56. **Kuras, L., P. Kosa, M. Mencia, and K. Struhl.** 2000. TAF-containing and

TAF-independent forms of transcriptionally active TBP in vivo. Science **288:**1244–1248.
57. **Kuras, L., and K. Struhl.** 1999. Binding of TBP to promoters in vivo is stimulated by activators and requires Pol II holoenzyme. Nature **399:**609–613.
58. **Larschan, E., and F. Winston.** 2001. The *S. cerevisiae* SAGA complex functions in vivo as a coactivator for transcriptional activation by Gal4. Genes Dev. **15:**1946–1956.
59. **Lee, D. K., J. DeJong, S. Hashimoto, M. Horikoshi, and R. G. Roeder.** 1992. TFIIA induces conformational changes in TFIID via interactions with the basic repeat. Mol. Cell. Biol. **12:**5189–5196.
60. **Lee, M., and K. Struhl.** 2001. Multiple functions of the nonconserved N-terminal domain of yeast TATA-binding protein. Genetics **158:**87–93.
61. **Lee, M., and K. Struhl.** 1995. Mutations on the DNA-binding surface of TATA-binding protein can specifically impair the response to acidic activators in vivo. Mol. Cell. Biol. **15:**5461–5469.
62. **Leurent, C., S. Sanders, C. Ruhlmann, V. Mallouh, P. A. Weil, D. B. Kirschner, L. Tora, and P. Schultz.** 2002. Mapping histone fold TAFs within yeast TFIID. EMBO J. **21:**3424–3433.
63. **Li, X.-Y., A. Virbasius, X. Zhu, and M. Green.** 1999. Enhancement of TBP binding by activators and general transcription factors. Nature **399:**605–609.
64. **Li, X. Y., S. R. Bhaumik, and M. R. Green.** 2000. Distinct classes of yeast promoters revealed by differential TAF recruitment. Science **288:**1242–1244.
65. **Liu, D., R. Ishima, K. I. Tong, S. Bagby, T. Kokubo, D. R. Muhandiram, L. E. Kay, Y. Nakatani, and M. Ikura.** 1998. Solution structure of a TBP-TAF(II)230 complex: protein mimicry of the minor groove surface of the TATA box unwound by TBP. Cell **94:**573–583.
66. **Maillet, L., C. Tu, Y. K. Hong, E. O. Shuster, and M. A. Collart.** 2000. The essential function of Not1 lies within the Ccr4-Not complex. J. Mol. Biol. **303:**131–143.
67. **Mermelstein, F., K. Yeung, J. Cao, J. A. Inostroza, H. Erdjument-Bromage, K. Eagelson, D. Landsman, P. Levitt, P. Tempst, and D. Reinberg.** 1996. Requirement of a corepressor for Dr1-mediated repression of transcription. Genes Dev. **10:**1033–1048.
68. **Muldrow, T. A., A. M. Campbell, P. A. Weil, and D. T. Auble.** 1999. MOT1 can activate basal transcription in vitro by regulating the distribution of TATA binding protein between promoter and nonpromoter sites. Mol. Cell. Biol. **19:**2835–2845.
69. **Nikolov, D. B., S. H. Hu, J. Lin, A. Gasch, A. Hoffmann, M. Horikoshi, N. H. Chua, R. G. Roeder, and S. K. Burley.** 1992. Crystal structure of TFIID TATA-box binding protein. Nature **360:**40–46.
70. **Nishikawa, J., T. Kokubo, M. Horikoshi, R. G. Roeder, and Y. Nakatani.** 1997. Drosophila TAF(II)230 and the transcriptional activator VP16 bind competitively to the TATA box-binding domain of the TATA box-binding protein. Proc. Natl. Acad. Sci. USA **94:**85–90.
71. **Pereira, L. A., J. A. van der Knaap, V. van den Boom, F. A. van den Heuvel, and H. T. Timmers.** 2001. TAF(II)170 interacts with the concave surface of TATA-binding protein to inhibit its DNA binding activity. Mol. Cell. Biol. **21:**7523–7534.
72. **Perez-Howard, G. M., P. A. Weil, and J. M. Beechem.** 1995. Yeast TATA binding protein interaction with DNA: fluorescence determination of oligomeric state, equilibrium binding, on-rate, and dissociation kinetics. Biochemistry **34:**8005–8017.
73. **Poon, D., A. M. Campbell, Y. Bai, and P. A. Weil.** 1994. Yeast TAF170 is encoded by MOT1 and exists in a TATA box-binding protein (TBP)-TBP-associated factor complex distinct from transcription factor IID. J. Biol. Chem. **269:**23135–23140.
74. **Poon, D., S. Schroeder, C. K. Wang, T. Yamamoto, M. Horikoshi, R. G. Roeder, and P. A. Weil.** 1991. The conserved carboxy-terminal domain of *Saccharomyces cerevisiae* TFIID is sufficient to support normal cell growth. Mol. Cell. Biol. **11:**4809–4821.
75. **Pugh, B. F.** 2000. Control of gene expression through regulation of the TATA binding protein. Gene **255:**1–14.
76. **Reddy, P., and S. Hahn.** 1991. Dominant negative mutations in yeast TFIID define a bipartite DNA-binding region. Cell **65:**349–357.
77. **Reese, J. C., L. Apone, S. S. Walker, L. A. Griffin, and M. R. Green.** 1994. Yeast TAFIIS in a multisubunit complex required for activated transcription. Nature **371:**523–527.
78. **Sanders, S. L., K. A. Garbett, and P. A. Weil.** 2002. Molecular characterization of *Saccharomyces cerevisiae* TFIID. Mol. Cell. Biol. **22:**6000–6013.
79. **Strubin, M., and K. Struhl.** 1992. Yeast and human TFIID with altered DNA-binding specificity for TATA elements. Cell **68:**721–730.
80. **Struhl, K.** 1999. Fundamentally different logic of gene regulation in eukaryotes and prokaryotes. Cell **98:**1–4.
81. **Taggart, A. K., and B. F. Pugh.** 1996. Dimerization of TFIID when not bound to DNA. Science **272:**1331–1333.
82. **Winston, F., K. J. Durbin, and G. R. Fink.** 1984. The SPT3 gene is required for normal transcription of Ty elements in *S. cerevisiae*. Cell **39:**675–682.
83. **Wyrick, J. J., F. C. Holstege, E. G. Jennings, H. C. Causton, D. Shore, M. Grunstein, E. S. Lander, and R. A. Young.** 1999. Chromosomal landscape of nucleosome-dependent gene expression and silencing in yeast. Nature **402:**418–421.
84. **Yamamoto, T., M. Horikoshi, J. Wang, S. Hasegawa, P. A. Weil, and R. G. Roeder.** 1992. A bipartite DNA binding domain composed of direct repeats in the TATA box binding factor TFIID. Proc. Natl. Acad. Sci. USA **89:**2844–2848.
85. **Zhou, Q. A., M. C. Schmidt, and A. J. Berk.** 1991. Requirement for acidic amino acid residues immediately N-terminal to the conserved domain of *Saccharomyces cerevisiae* TFIID. EMBO J. **10:**1843–1852.